

April 2018

Solar Powered Urban Pollution Mapping

Mateo Carvajal
Worcester Polytechnic Institute

Follow this and additional works at: <https://digitalcommons.wpi.edu/mqp-all>

Repository Citation

Carvajal, M. (2018). *Solar Powered Urban Pollution Mapping*. Retrieved from <https://digitalcommons.wpi.edu/mqp-all/662>

This Unrestricted is brought to you for free and open access by the Major Qualifying Projects at Digital WPI. It has been accepted for inclusion in Major Qualifying Projects (All Years) by an authorized administrator of Digital WPI. For more information, please contact digitalwpi@wpi.edu.



WPI

Solar Powered Urban Pollution Mapping

A Major Qualifying Project
Submitted to the Faculty of
WORCESTER POLYTECHNIC INSTITUTE
In partial fulfillment of the requirements for the
Degree of Bachelor of Science in
Electrical and Computer Engineering

By
Mateo Carvajal

Report Submitted to:

Professor Susan M. Jarvis
Worcester Polytechnic Institute

April 24, 2017

Project Number:
MQP-SMJ-ABGW

Worcester

This report represents work of WPI undergraduate students submitted to the faculty as evidence of a degree requirement. WPI routinely publishes these reports on its web site without editorial or peer review. For more information about the projects program at WPI, see <http://www.wpi.edu/Academics/Projects>.

Abstract

Eighty percent of all urban areas in the world report air pollution levels higher than the standards deemed safe by the World Health Organization. This project explores the creation of a prototype that can granularly measure air quality in urban areas. The prototype measures carbon monoxide, nitrogen dioxide, sulfur dioxide, hydrogen sulfide, ozone and particulate matter. The prototype also acquires the geographical position of the measurement and reports the data wirelessly to a database. This approach can enable governments and citizens to foster improvements to urban environments that have high levels of pollution.

Acknowledgments

I would like to thank Prof. Susan Jarvis for her guidance throughout the project; her contributions have enhanced this project in many ways. Kayleah Griffen for creating the power component for the project, a major and key part of the project. Her willingness to integrate it to the system has resulted in a very rewarding outcome. I would also like to thank those behind the scenes, who helped move the project forward, Ching-Hsiang Chen and other close friends who provided the much needed inspiration and support in this endeavor.

Table of Contents

Abstract	ii
Acknowledgments.....	iii
Table of Contents	iv
Table of Figures	v
1. Introduction	1
2. Background.....	3
3. Design.....	6
3.1 Sensors	6
3.2 Wireless Data Transmission and GPS.....	13
3.3 Microcontroller.....	13
3.4 Solar Power and Battery.....	14
4. Implementation.....	15
4.1 Electrochemical Sensors	15
4.2 Particulate Matter Sensor	20
4.3 FONA 808.....	24
4.4 Atmega 2560	27
4.5 Solar Power and Battery.....	29
4.6 Final Hardware Layout.....	29
5. Results	33
6. Conclusion and Recommendations	38
7. Bibliography	39
8. Appendix	42
Appendix A: Solar Power and Battery	42
Appendix B: Bill of Materials (BOM)	59
Appendix C: ULPSM Schematic [9].....	60
Appendix D: Code Listing	61
Main.cpp	61
Mqpdef.h.....	62
SpecSensorCode.cpp	65
pmSensorCode.cpp	68
Power.cpp	71
Ubidots.cpp.....	75
Appendix E: MATLAB Practical Model Parameter Extraction Code	77
Appendix F: MATLAB Practical Model Characteristic Curve Plotting Code	78
Appendix G: MATLAB Simulink Practical Model Solar Panel with DC to DC Converter	81
Appendix H: Maximum Power Point Tracking Code written in MATLAB.....	82
Appendix I: Additional Research.....	84

Table of Figures

Figure 1 - Luftmeßnetz Hamburg [8].....	4
Figure 2 - Concept of operation for distributed pollution monitoring system.....	5
Figure 3 – High level Design of the System.....	6
Figure 4 - Spec sensor general design [9].....	7
Figure 5 - SPEC Sensor	7
Figure 6 - SPEC Ultra Low Power Sensor Module (ULPSM).....	8
Figure 7 - Shinyei Technology Particulate Matter Sensor [15].....	12
Figure 8 – Overall System Signal Diagram	15
Figure 9 - SPEC ULPSM Layout.....	16
Figure 10 - Spec Sensor Connection to Buffer Amplifier	17
Figure 11 - ULPSM Vgas and Vref Output	19
Figure 12 - NTC Murata NCP18WM474J03RB Thermistor Layout.....	19
Figure 13 - Shinyei Particulate Matter Sensor Layout.....	20
Figure 14 - Extracting Two Bytes from Buffer	21
Figure 15 - Pulse Occupancy Ratio vs Weight Concentration [17].....	24
Figure 16 - FONA 808 3G and GPS Module Layout.....	25
Figure 17 - UbidotsFONA Modifications for GPS Acquisition.....	27
Figure 18 - Oscillator Connection to Atmega2560.....	28
Figure 19 - Voltage Regulators in PCB Design.....	30
Figure 20 - Overall Schematic without Solar Power and Battery Design	31
Figure 21 - Top of PCB	32
Figure 22 – Bottom of PCB	32
Figure 23 - Temperature Sensor Results.....	33
Figure 24 - Results from PM Sensor Message.....	35
Figure 25 - GPS Response	35
Figure 26 - HTTP Post Command and FONA Response	36
Figure 27 – Sulfur Dioxide Ubidots Results.....	36
Figure 28 – Final Prototype of our solar powered pollution measurement system	37
Figure 29 - Voltage vs Power Curve for 2W Solar Panel.....	45
Figure 30 - Basic Layout of DC/DC Boost Converter.....	46
Figure 31 - Inductor Analysis	48
Figure 32 - Solar Charging Boost Converter Topology.....	48
Figure 33 - Voltage Follower and Voltage Divider Circuit.....	50
Figure 34 - Full Solar Charging System Schematic.....	51
Figure 35 - Solar Panel Practical Model.....	53
Figure 36 - Characteristic IV and PV Curves for Solar Panel	54
Figure 37 –Duty Cycle Simulations.....	55
Figure 38 - Complete Prototype.....	56
Figure 39 - The IV and PV Characteristic Curves for the Solar Panel	57
Figure 40 - Maximum Power Point Tracking Test Case	57

Figure 41 - Voltage Varying as a Result of Irradiance Level Changing	58
Figure 42 – Wireless Technologies Comparison	85

1. Introduction

Air pollution is a grave health problem. In 2005, The World Health Organization (WHO) estimated that 2 Million lives were being lost prematurely due to air pollution [1]. In 2016, The Global Burden of Disease, a global research program, estimated that the deaths due to outdoor and household pollution were 5.5 Million [2]. Both studies are alarming. The future looks even more distressing. The Organization for Economic Co-operation and Development (OECD), in a 2012 report, estimated that by the year 2050, the leading cause of premature deaths would be air pollution, ahead of unsafe water and sanitation [3].

Urban areas are at the frontline of this battle. The WHO reported that 80% of all urban areas record measurements of pollution that are higher than those recommended for human health [1]. In urban areas in Asia, the figure rises to 98%.

The main urban air pollutants, also known as *primary pollutants* as they are produced directly from the source are Nitrogen Oxides (NO_x), Sulfur Oxide, Carbon Monoxide, Lead and Particulate Matter (PM). *Secondary pollutants* are those that result from chemical reactions in the air between the primary pollutants and naturally occurring gases for example Ozone (O³), Sulfuric Acid (H₂SO₂) and Nitric Acid (HNO₃). Excess of these pollutants can be directly attributed to human activity.

Carbon monoxide is primarily a result of human activity. Mobile sources account for the biggest fraction of carbon monoxide emissions in the US. Mobile sources are regarded as those that can move, for example, vehicles (cars & trucks) airplanes, locomotives and ships. Mobile sources, especially cars and trucks, account for up to 95% of the carbon monoxide emissions in urban areas [4]. CO is an odorless and colorless gas. It is a result of fossil fuel combustion. When inhaled, CO is carried in the red blood cells that normally carry oxygen. This results in less oxygen reaching the brain and other organs. Resulting in chest pain and headaches at low concentrations. At very high concentrations, carbon monoxide is lethal. In the US, the Occupational Safety and Health Administration limits the exposure to 50 ppm.

Nitrogen oxides are the result of combustion processes of nitrogen bearing coals and oil. When the fuels combust the nitrogen particles are released. These particles form N₂ or NO_x. The latter having negative effects on the environment and other living beings. Exposure to NO₂ causes inflammation of the nose and throat. Long-term exposure increases the risk of respiratory conditions such as asthma, bronchitis or pneumonia and increases the allergic response to allergens [5]. Concentrations of 10-20 ppm causes irritation to the throat. 25-50 ppm can cause pulmonary edema, an increase accumulation of fluids in the lungs. 100 ppm or higher can cause death from asphyxia from liquids in the lungs.

Hydrogen sulfide is a toxic and flammable gas. At low concentrations (10-50 ppm), H₂S irritates soft tissue like eyes and throat. Long exposure can cause eye inflammation, headache insomnia and fatigue. In addition, moderate concentrations (50-320 ppm) can cause coughing, difficulty to breathe (pulmonary edema), nausea and vomiting [6]. High concentrations (>400 ppm) can cause, shock, convulsions, rapid

unconsciousness within a few breaths, or even a single breath. The largest industrial source of hydrogen sulfide are petroleum refineries, which liberate sulfur from petroleum by mixing it with hydrogen. This results in H₂S. Hydrogen Sulfide is also released from biological decay.

Sulphur dioxide anthropogenic emissions are mainly the result of the burning of fossil fuels such as coal, oil and natural gas. Coal accounts for 50 percent of annual emissions, oil 25 percent. Volcano eruptions can also release high levels of sulfur dioxide. High concentrations of SO₂ can cause inflammation of soft tissue such as the eyes, nose, throat and lungs.

Ozone is an important compound in the ozone layer, where it absorbs ultraviolet radiation and protects the earth. On the ground level, ozone is harmful to health. It is mainly a result of reactions of pollutants emitted from the burning of fossil fuels.

Particulate matter is a mix of solid and liquid droplets that are found in the air. Some of the particles are large enough for the human eye to see concentrations of them. Others are small enough that they can only be seen using an electron microscope.

Different cities suffer from different pollutants. Policies, population density, per capita emissions, wind direction and topographic barriers all take part in determining the pollutants that affect a given urban area. In Delhi, India the annual mean concentration of PM₁₀ (particles 10- $\mu\text{g m}^{-3}$ or less) is 240- $\mu\text{g m}^{-3}$, 12 times more than the 20- $\mu\text{g m}^{-3}$ level set by the WHO as safe. In the UK nitrogen oxides (NO_x) are above the permitted limits in 40% of Britain's local authorities. This is in part due to past legislations that incentivized the use of diesel powered vehicles over gasoline ones. However, British PM₁₀ is within the permitted values. In New York, the high population density allows for a greater use of public transportation. In addition, no significant topographic barriers are present, allowing the wind to blow the pollutants away from their source.

Despite being at a moment in time where scientists know how air pollution is produced, how it affect us and have taken action to set goals for emissions, the rate at which people die prematurely has not yet shown signs of decline. More has to happen in order to revert this lethal trend.

This project aims to provide an affordable, portable and self-reliant tool to monitor pollution. Providing data to create awareness and inspire targeted corrective actions by local governments and citizens.

2. Background

Air pollution is dispersed uniquely in different environments. Each city, for example, has different building sizes, wind speed, direction, topographies, traffic flows, and geographical location. Scientists have struggled to measure pollution effectively across cities. This is mainly due to the cost of implementing a citywide monitoring infrastructure. For this reason, mathematical models have been developed to understand the dispersion of pollution around streets and buildings with limited data sources.

Table 1 – Air Quality Monitoring Stations in Cities around the Globe

City, Country	Population (Million)	Area (km²)	Number of Monitoring Stations
New York City, USA	8.5	789	150
London, UK	8.7	1,738	33
Bogota, Colombia	8.0	1,775	14
Mexico City, Mexico	8.8	1,485	30
Delhi, India	19.0	1,484	30
Hamburg, Germany	1.8	755	16

Currently, air quality is measured at city levels. In developed countries, for example, monitoring stations are found throughout urban areas. The data is then used to support and enforce environmental policies. The stations are large in order to house high precision measurement equipment; in Figure 1 one can observe one of these stations in Hamburg, Germany. The pictured station is located on Stresemannstraße. It has been recording data since October 24, 1991. It currently records data on Air pollutants such as particulate matter (PM10) nitrogen oxide, nitrogen dioxide and nitrogen oxides at different heights, mainly 1.5, 3.5, 4.0 meters above ground [7]. Since this station started monitoring It has changed the gases it can sense, mainly due to the shifting challenges that cities face with improvements in new technologies.

Different cities have different capabilities to monitor and control air quality. New York uses 150 monitoring stations to control air quality. London has at least a monitoring station for each of each of its 33 boroughs. Delhi has 28 monitoring stations. Bogota, Colombia uses 14 stations. Mexico City, 30. Hamburg, 16. What is particularly interesting is how many stations one can find in some cities and how few you can find in others as seen on the Table 1. Some cities are lacking the infrastructure to monitor and control air pollutants.

All the data that is being collected can be used to save lives. Nonetheless, more data could be collected in order to create an extensive database that can be used in helping plan urban spaces effectively to reduce the negative effects of air pollution on citizens.

Fortunately, at this day and age technology has become accessible in terms of development and costs. An *army* of small, embedded systems that provide extensive data to understand citywide air quality measurements is now feasible.



Figure 1 - Luftmeßnetz Hamburg [8]

The goal of this project is to do exactly that. Develop a system that will monitor air quality in urban areas with the geographical coordinates of the measurement and relying on its surrounding to harvest energy. Then transmit the data through a wireless signal. With the help of many of these devices a centralized system will be able to make sense of all the data and display it accordingly. The vision for this development is to provide a tool for city planners to understand how pollution is distributed in the city and empower them to take action to reduce pollution in critical areas in a cost effective manner.

The project also has in mind the general population, allowing them to use the devices to measure air quality. Moreover, providing them with access to the data and information of the risks in order to inspire change on their street, neighborhood or the city level. Michael Brauer, a Professor at the School of Population and Public Health at the University of British Columbia, emphasizes that access to information on the health

impacts of air pollution will catalyze the shift of using dirtier energy sources to more environmentally friendly ones.

Mobile Network of Devices

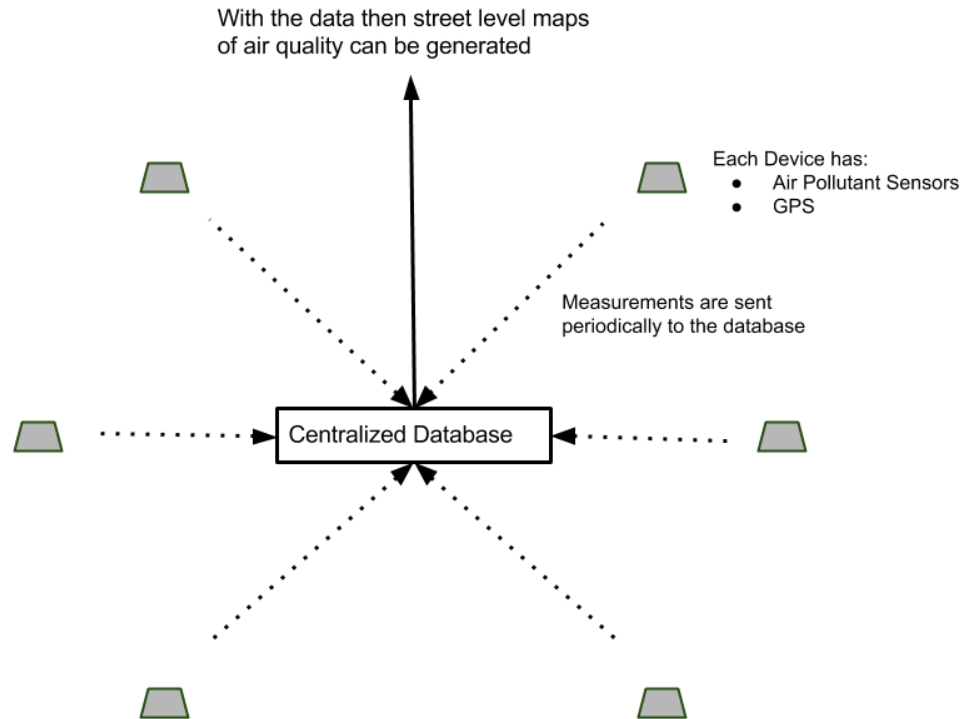


Figure 2 - Concept of operation for distributed pollution monitoring system

This project is different from the current methods of measuring air pollution as it will allow a granular approach to measuring and hopefully, controlling the substances in the air that affect human health. This project also contains an important component of community participation that seeks to raise awareness of the effects of pollutants in health and to allow individuals to create campaigns to reduce the pollution in their areas of interest.

3. Design

The goals of this project is to create a system that will measure six of the substances that burden urban areas air quality. Namely, particular matter, carbon monoxide, nitrogen dioxide, sulfur dioxide, hydrogen sulfide and ozone. In order to record the geographical location we will implement a GPS module. For the transmission of the data a wireless signal will be used. The device will also harvest the energy it needs to run from sunlight. Figure 3 displays a high level view of the entire system.

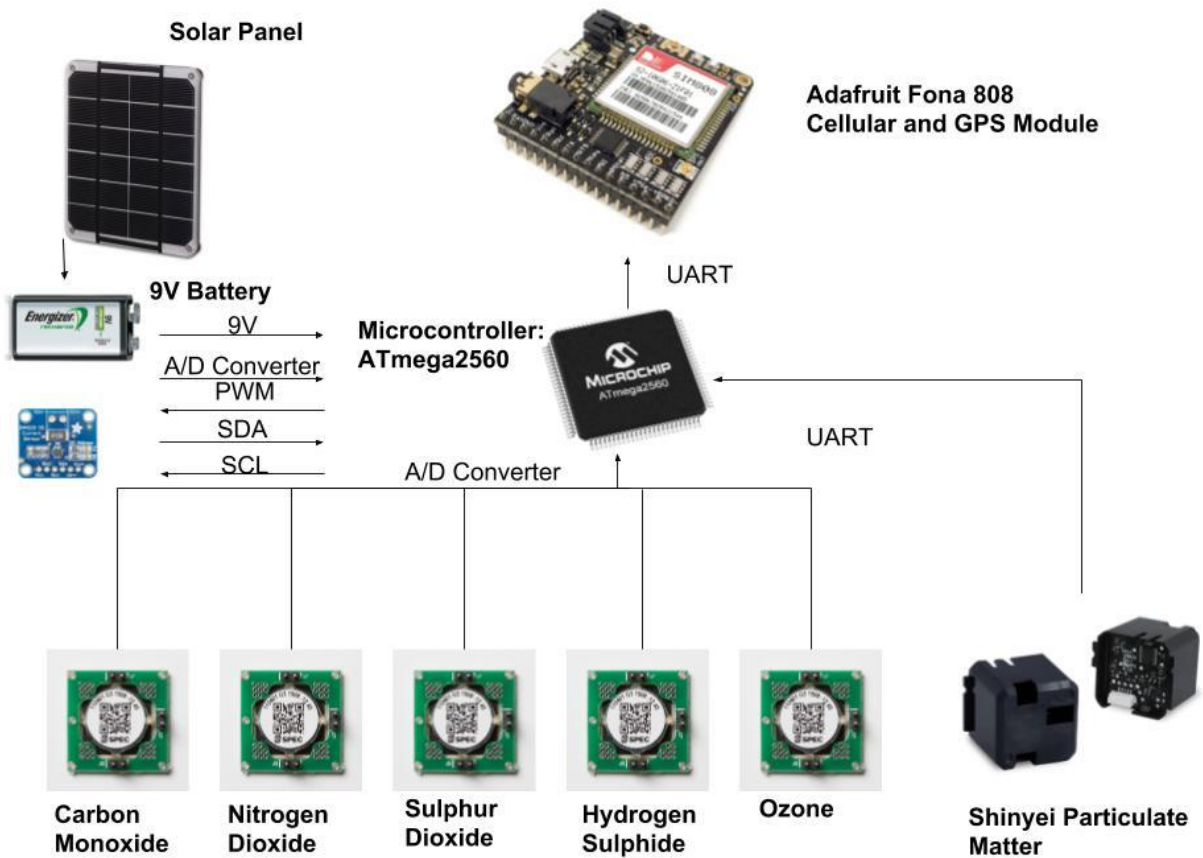


Figure 3 – High level Design of the System

3.1 Sensors

SPEC Sensors

For the development of this project, we investigated sensors that could measure the concentration of the different air pollutants. For the size and reliability, we chose SPEC sensors for measuring CO, NO₂, H₂S, SO₂ and O₃. All of these sensors are

amperometric gas sensors; they generate a current proportional to the concentration of a gas. The sensor, as seen in Figure 4, has a catalytic metal (sensing electrode) that is selected for each to optimize the reaction of each target gas. This reaction produces or attracts electrons that then generate a current.

The output of these sensors is a current signal, which by nature is analog. For this reason, circuitry was designed to use the current to generate a voltage with a resistor and then map the voltage variations to calculate the concentration of the gasses.

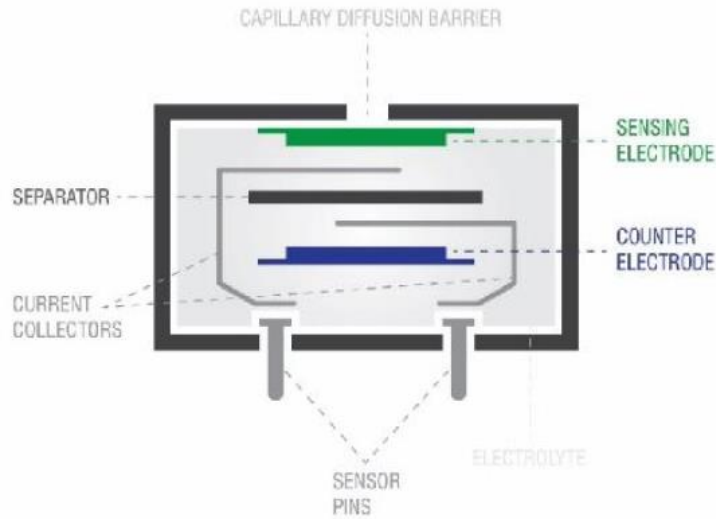


Figure 4 - Spec sensor general design [9]

For this project we used the analog sensor modules (as seen on Figure 6) provided by SPEC to use with their sensors (as seen on Figure 5). The analog sensor modules uses two pairs of operational amplifiers to generate an output voltage that is proportional to the concentration of the gas while maintaining the bias voltage to the sensor.

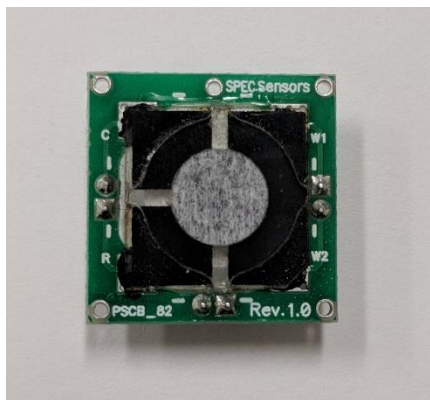


Figure 5 - SPEC Sensor

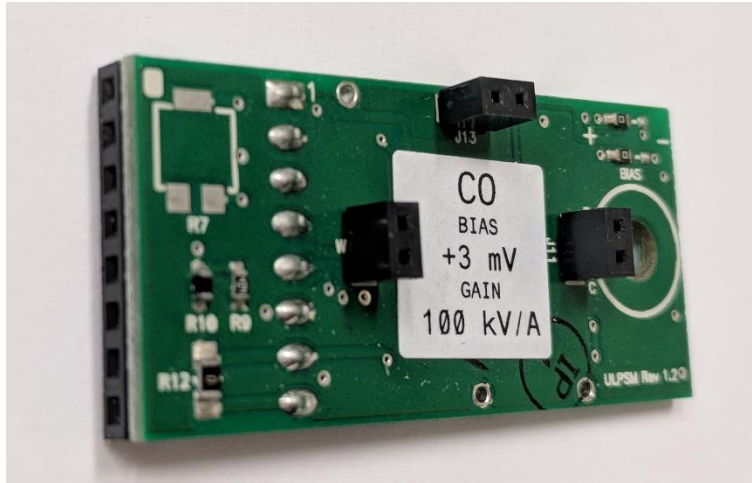


Figure 6 - SPEC Ultra Low Power Sensor Module (ULPSM)

The analog sensor modules operate at 3V and have under 45 μ W of power consumption making them low power. These modules feature a temperature sensor and allow for easy sensor replacement, in case of damage.

The gas concentration for each gas is calculated with Equation 1.

$$Concentration_{Gas} (ppm) = \frac{1}{M} * (V_{gas} - V_{gas_0}) \quad \text{Eq. 1 [10]}$$

Where concentration is measured in parts per million (ppm). V_{gas} is the output voltage of the gas signal and V_{gas_0} is the output voltage of the gas signal in an environment free of the target gas. M is the sensor calibration factor (V/ppm) and is calculated in the following way:

$$M \left(\frac{V}{ppm} \right) = SensitivityCode \left(\frac{nA}{ppm} \right) * TIA\ Gain \left(\frac{kV}{A} \right) * 10^{-9} \left(\frac{A}{nA} \right) * 10^3 \left(\frac{V}{kV} \right) \quad \text{Eq. 2 [10]}$$

Where the sensitivity code is printed on each sensor's label. The TIA Gain is the gain of the trans-impedance amplifier (TIA) of the analog sensor module. SPEC Sensors provides different modules for the different analytic gases. The TIA Gain for each sensor are provided by the manufacturer and are displayed on Table 2.

Table 2 - Trans-impedance Amplifier Gain [9]

Target Gas	TIA Gain (kV/A)
Carbon Monoxide	100
Nitrogen Dioxide	499
Sulfur Dioxide	100
Hydrogen Sulfide	49.9
Ozone	499

The manufacturer of the sensors has registered that its sensor response have a predictable fluctuation with changes in temperature. The sensor results must be adjusted to account for the normal fluctuation. Tables 2 through 6 have Temperature coefficients for each target gas.

Table 3 – Carbon Monoxide Temperature Compensation [10]

Temperature Range	Temp Compensation Coefficient
-20°C to 0°C	0.06 ppm/°C
0°C to 25°C	0.3 ppm/°C
25°C to 40 °C	1.4 ppm/°C

Table 4 – Nitrogen Dioxide Temperature Compensation [11]

Temperature Range	Temp Compensation Coefficient
-20°C to 30°C	0 ppm/°C
30°C to 50°C	0.0066 ppm/°C

Table 5 – Sulfur Dioxide Temperature Compensation [12]

Temperature Range	Temp Compensation Coefficient
-20°C to 0°C	0.012 ppm/°C
0°C to 25°C	0.056 ppm/°C
25°C to 40 °C	0.46 ppm/°C

Table 6 - Hydrogen Sulfide Temperature Compensation [13]

Temperature Range	Temp Compensation Coefficient
-20°C to 0°C	0.0022 ppm/°C
0°C to 25°C	0 ppm/°C
25°C to 40 °C	0.003 ppm/°C

Table 7 - Ozone Temperature Compensation [14]

Temperature Range	Temp Compensation Coefficient
-20°C to 30°C	0 ppm/°C
30°C to 50°C	0.0066 ppm/°C

In order to account for the temperature compensations equation 3 can be used.

$$\begin{aligned}
 & \text{Concentration}_{Gas} \text{ (ppm)} \\
 &= \frac{1}{M} * (V_{gas} - V_{gas_0}) + \text{TempCompen} \left(\frac{\text{ppm}}{^\circ\text{C}} \right) * \text{Temp}(^\circ\text{C}) \quad \text{Eq. 3 [10]}
 \end{aligned}$$

When using the SPEC sensors it is important to note that the sensors have cross sensitivity between the different analytic gases, they are minor in relation to the analyzed gas. This means that a sensor for a specific gas shows a response when other gases increase their concentrations. Each type of sensor reacts differently to different gases. Tables 7 – 11 display the information provided by SPEC Sensors.

Table 8 - Carbon Monoxide Cross Sensitivity [10]

Gas	Applied Concentration (PPM)	Typical Response (PPM CO)
Carbon Dioxide	5000	< 1
Hydrogen	100	17
Methane	3000	< 1
Ammonia	100	< 1
Nitrogen Dioxide	10	< 1
Hydrogen Sulfide	25	< 1
Carbon Monoxide	400	400
Ozone	5	< 1
Sulfur Dioxide	20	< 1
Chlorine	10	< 1
n-Heptane	500	< 1

Tolouene	200	< 1
Isopropyl Alcohol	200	1.3
Acetone	200	< 1

Table 9 - Nitrogen Dioxide Cross Sensitivity [11]

Gas	Applied Concentration (PPM)	Typical Response (PPM NO2)
Nitrogen Dioxide	5	5
Hydrogen Sulfide	5	< 0.02
Ozone	1	< 0.1
Nitric Oxide	5	< 0.1
Sulfur Dioxide	5	< 0.02
Carbon Monoxide	100	< 0.2
Chlorine	10	< 0.5

Table 10 - Sulfur Dioxide Cross Sensitivity [12]

Gas	Applied Concentration (PPM)	Typical Response (PPM SO2)
Sulfur Dioxide	20	20
Hydrogen Sulfide	25	142.3
Nitric Oxide	50	90.5
Carbon Monoxide	400	7.3
Ozone	5	-3.3
Chlorine	10	-2.8
Nitrogen Dioxide	10	1.4
n-Heptane	500	-0.7
Methane	500	0.7
Ammonia	100	< 0.2

Table 11 - Hydrogen Sulfide Cross Sensitivity [13]

Gas	Applied Concentration (PPM)	Typical Response (PPM H2S)
Hydrogen Sulfide	25	25
Chlorine	10	-2.2
Nitrogen Dioxide	10	-2.0
Sulfur Dioxide	20	1.7
Nitric Oxide	50	1.2
Carbon Monoxide	400	1.1
Ozone	5	-0.9
Methane	500	0.1

Ammonia	100	0.1
n-Heptane	500	< 0.05

Table 12 - Ozone Cross Sensitivity [14]

Gas	Applied Concentration (PPM)	Typical Response (PPM O3)
Ozone	5	5
Hydrogen Sulfide	25	-5
Chlorine	10	10
Nitrogen Dioxide	5	5
n-Heptane	1000	< -0.1
Carbon Monoxide	400	< 0.05
Methane	500	< 0.05

Shinyei Sensor

For measuring the concentration of particulate matter (PM), we required a different sensor since we are no longer measuring a gas but the presence of particles in the air. For this application, we chose the PPD71 of Shinyei Electronics, as seen in Figure 7. This sensor measures PM by using a light scattering method. It has a led that shines light through the space where the air is and then uses a sensor that measures how much light is scattered from the source. This measurement is then used to calculate the concentration of particulate matter. The sensor takes care of this calculations and outputs the mass concentration ($\mu\text{g}/\text{m}^3$) and a pulse occupancy ratio (percentage) corresponding to the particle counts per volume. The pulse occupancy ratio is available from the sensor for particles greater than 0.5, 0.7, 1.0 and 2.5 μm .

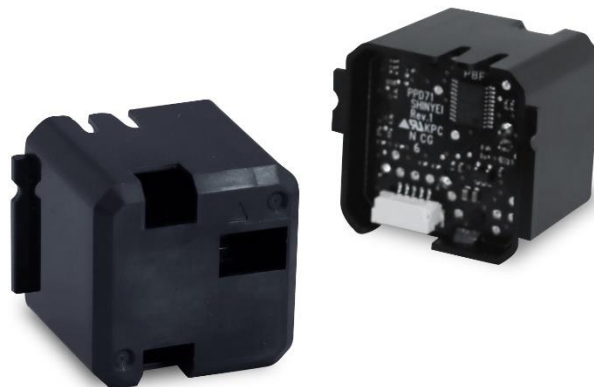


Figure 7 - Shinyei Technology Particulate Matter Sensor [15]

3.2 Wireless Data Transmission and GPS

Wireless data transmission is a key feature of this project. It will reduce the setup time of the system and will allow the system to be mobile since no wired infrastructure is needed. Also, since urban environments have a predominant and extensive cover of 3G network. The system can be relocated easily if necessary. Note: the system is not recommended to be used on moving vehicles as the gas concentrations can change faster than the sensors are able to measure. Nonetheless, the system could be placed on a moving vehicle and it can record data when the vehicle is stationary for longer periods.

In order to report the location of the data the integration of a Global Navigation Satellite System (GNSS) capability into the system is required. GNSS or Global Navigation Satellite System is a satellite system that is used to determine the location of a specific device around the globe. A GNSS chip determines its location by receiving signals from at least four different satellites and then computing the transmission delay of the four satellites signals to determine the exact position on the globe.

There are four different GNSS constellations or satellite systems. There is Global Positioning System (GPS), GLONASS, BeiDou and Galileo. GPS is the most widely used system. It currently has 31 satellites orbiting earth. The GPS system is maintained by the United States. On the other hand, GLONASS, translated to Global Navigation Satellite System holds 23 satellites in operation and it is maintained by Russia. BeiDou is the Chinese version; it is only operational in China's region [16], although global coverage is scheduled for 2020. Last, Galileo has not yet fully operational capability, and changes to it are expected.

For our project the accuracy of GPS and GLONASS are practically the same. GLONASS is especially better at extreme latitudes, far south and far north, due to the position of its satellites. For this project, using GPS is sufficient.

For acquiring the GPS signal and connecting to the cellular network we will use the Adafruit FONA 808 3G and GPS breakout board. The FONA 808 is capable of receiving and posting http requests as well as acquiring the GPS signal. This module is also capable of making and receiving calls and text messages. In order to use this device a 3G and GPS antenna are required. This module also requires a sim card and a dedicated battery in order to operate.

3.3 Microcontroller

Last we need to select a microcontroller that can handle all of the requirements set by the other components of the project. Each SPEC sensor require two analog inputs, we have 5 sensors, and hence we need 10 analog inputs. It is also highly desirable that we can use variable reference voltages to adjust the reference to obtain the highest accuracy of the readings on the microcontroller. For the particulate matter sensor we require a UART receiver on the microcontroller to receive the data. And for the FONA 808, 3G and GPS module requires a UART receiver and a transmitter.

We also took into consideration the learning curve required to use the microcontroller. We chose the ATmega2560 that is used on the Arduino Mega development board since there is widely available documentation in its use.

The ATmega2560 is an 8-bit microcontroller that features 16 channel 10-bit ADC (Analog to Digital Converter) channels. This means that the ATmega, although 8-bit can access the 10 bit resolution in two operations. For our application we will left adjust the reading and use 8-bit precision. The ATmega also has variable reference voltages options. One can either use the default, set to 3.3V, or set VREF to 1.1V, 2.56V or to an external reference voltage.

3.4 Solar Power and Battery

In order to develop the power system we worked with Kayleah Griffen to develop a power system that could supply sufficient energy to our components. Please refer to *Appendix A* Appendix A: Solar Power and Battery to find more information on the design of this component.

The solar power system developed and found in Appendix A requires commands from the microcontroller in order to function. The solar power system needs to connect to a common ground, use I²C (SDA, SCL), a pulse with modulation(PWM) pin, an analog input and must provide power to the power rail of the pollution system.

4. Implementation

Now that we have researched and selected the different components for the project. Now, it is time to start the implementation. We will implement and write the code for each component individually and then we will proceed to merge all of the components into an integrated program. Figure 8 shows how the different components interface with the ATmega2560 microcontroller.

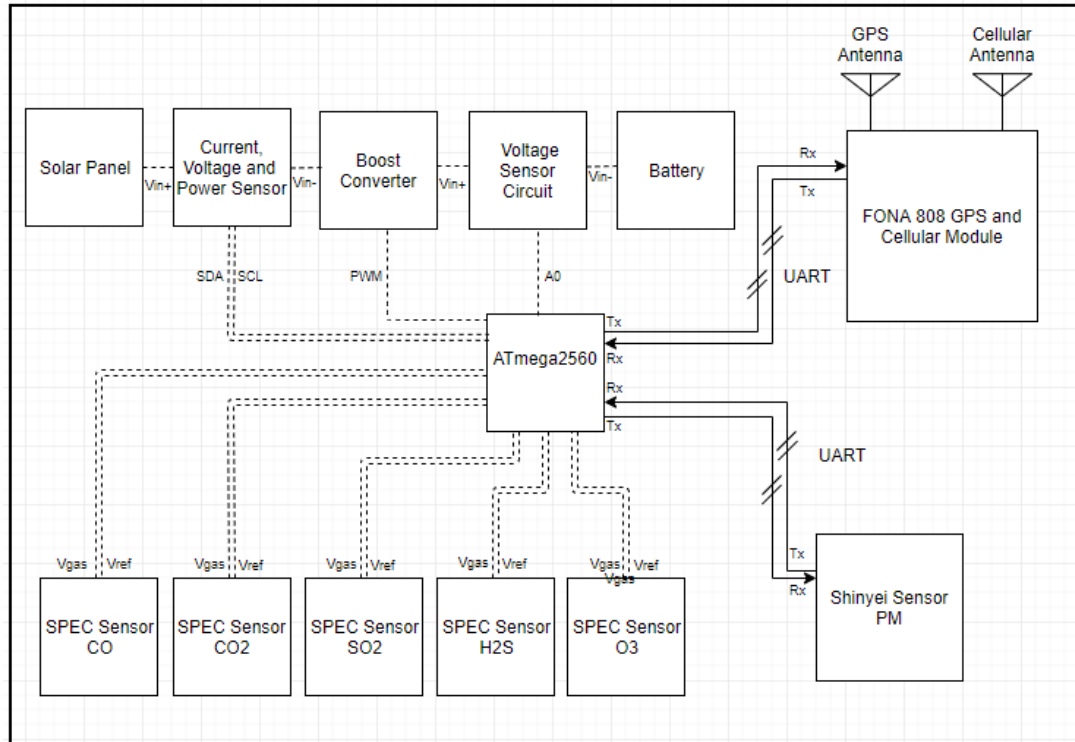


Figure 8 – Overall System Signal Diagram

4.1 Electrochemical Sensors

Hardware

To start the implementation of the SPEC sensors we first need to understand the physical layout of the SPEC Ultra-Low Power Analog Sensor Module (ULPSM) to which the sensors are connected. Each ULPSM has a different internal wiring to configure the different trans-impedance gains for the different sensors. However, they all have the same configuration of outputs as seen on Figure 9. The descriptions of the pins can be found on Table 13.

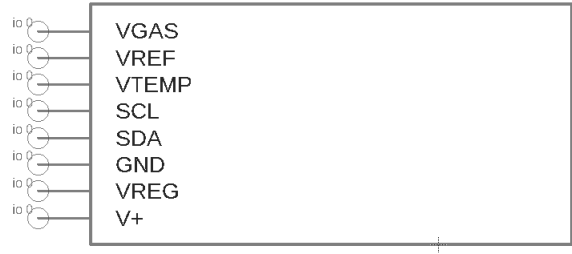


Figure 9 - SPEC ULPSM Layout

Table 13 – SPEC ULPSM Pin Descriptions [10]

PIN Name	PIN Num.	Type	Description
Vgas	1	Output	Proportional to the gas concentration
Vref	2	Output	Reference voltage. Equivalent to zero for Vgas. Note: It must be connected to a buffer amplifier as it has a high impedance output
Vtemp	3	Output	Proportional to the temperature
SCL	4	Not used	
SDA	5	Not used	
GND	6	Input	Universal Ground for power and signal
Vreg	7	Input	Supply Voltage 2.7V to 3.3V
V+	8	Input	Supply Voltage 2.7V to 3.3V

The ULPSM are powered through the 3V rail. Note that pins 8 & 9 can both power the system. Connecting only one is sufficient. Vref is connected to a buffer amplifier as seen on Figure 10. Next, we will assign the outputs Vref and Vgas pins to the ATmega pins. Please refer to Table 14. Please note that we use the Temp connection of the Ozone ULPSM only as we assume that the temperature measured there will be an accurate representation of the temperature around all other sensors. Later we will show the development of a PCB board with the Atmega 2560 microcontroller so the last column pin numbers in Table 14 become relevant.

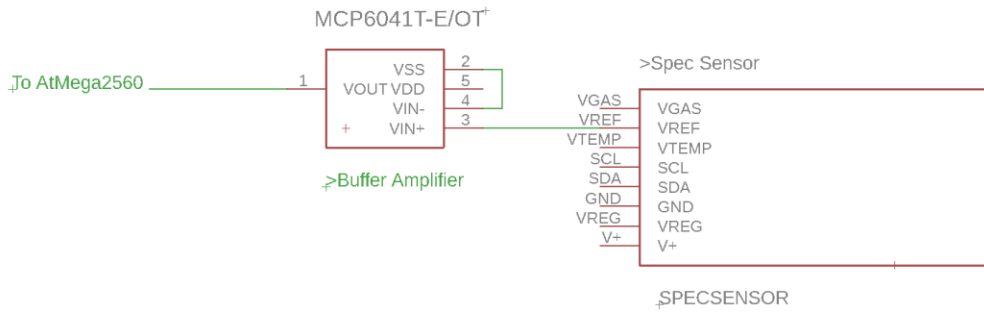


Figure 10 - Spec Sensor Connection to Buffer Amplifier

Table 14 - SPEC Sensor Pin Assignments

Gas	ULPSM Pin	Arduino Label	Arduino Mega Pins	Atmega 2560 pins (Custom PCB)
Carbon Monoxide	Vref	A0	54	55
	Vgas (Buffer out)	A1	55	54
Nitrogen Dioxide	Vref	A2	56	57
	Vgas (Buffer out)	A3	57	56
Sulfur Dioxide	Vref	A4	58	59
	Vgas (Buffer out)	A5	59	58
Hydrogen Sulfide	Vref	A6	60	61
	Vgas (Buffer out)	A7	61	60
Ozone	Vref	A8	62	63
	Vgas	A9	63	62
	Vtemp (Buffer out)	A10	64	64

Software

In order to calculate the concentration of each specific gas at runtime we will use Equation 1. However, we will hardcode the value of the inverse of the calibration factor M to reduce the amount of calculations needed. For this process, we will use Equation 4, derived from Equation 2. The sensitivity codes are printed behind each sensor and the TIA gains are listed on Table 2.

$$M_X^{-1} \left(\frac{\text{ppm}}{\text{V}} \right) = \frac{1}{\text{SensitivityCode} \left(\frac{\text{nA}}{\text{ppm}} \right) * \text{TIA Gain} \left(\frac{\text{kV}}{\text{A}} \right) * 10^{-9} \left(\frac{\text{A}}{\text{nA}} \right) * 10^3 \left(\frac{\text{V}}{\text{kV}} \right)} \quad \text{Eq. 4}$$

In our system implementation, the following is the result of the inverse calibration factors. Please note that the Sensitivity codes will change with every sensor.

Table 15 - Results of the Inverse Calibration Factor

Analytic Gas	Sensitivity Code	TIA GAIN	1/M (ppm/V)
Carbon Monoxide	4.44	100	2252.252
Nitrogen Dioxide	-23.81	49.9	-841.667
Sulfur Dioxide	36.58	499	54.784
Hydrogen Sulfide	-267.86	100	-37.333
Ozone	-72.04	499	-27.818

In the header file in the code we have hardcoded the results of Table 15 for each sensor under the names SPEC_CONSTANT_1_M_[GAS]. Where [GAS] is replaced by the chemical notation for each of the compounds. This can be found in the '[mqpdef.h](#)' file.

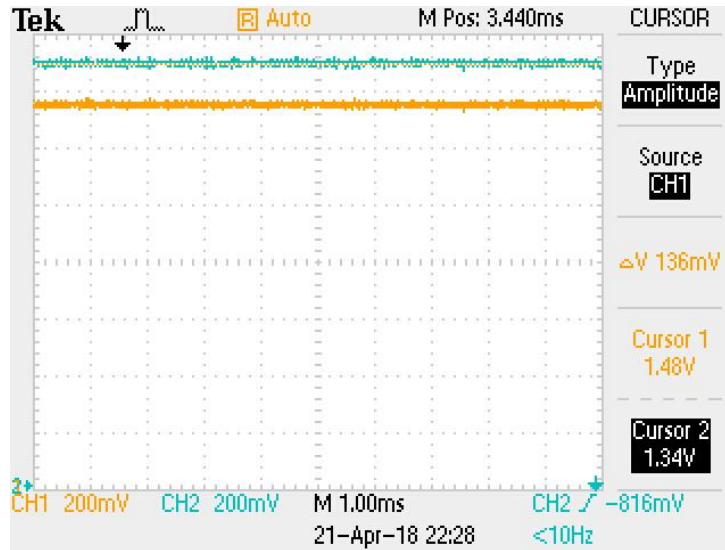


Figure 11 - ULPSM Vgas and Vref Output

From the ULPSM we can also extract the ambient temperature. Pin Vtemp on the ULPSM. This pin is internally connected to an NTC Thermistor as seen on Figure 12. This type of thermistors decrease its resistance as temperature increases. By measuring V_{TEMP} and having the thermistor parameters we can calculate the temperature T in Kelvin from Equation 5. In our software implementation, we subtracted additionally 273 to the result to T to obtain the result in Celsius.

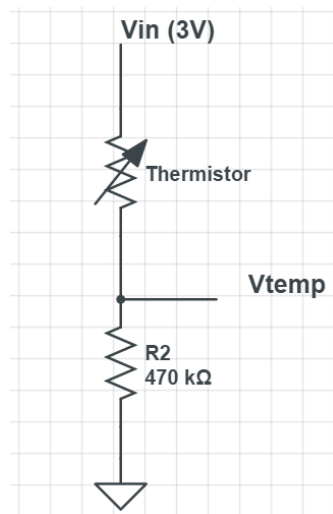


Figure 12 - NTC Murata NCP18WM474J03RB Thermistor Layout

Table 16 - Thermistor

NTC Thermistor	Values
BCoefficient	4600
T ₀	298[K]
V _{in}	3 [V]

$$\frac{1}{T} = \frac{1}{T_0} + \frac{1}{B} \ln\left(\frac{V_{in}}{V_{TEMP}} - 1\right) \quad \text{Eq. 5}$$

4.2 Particulate Matter Sensor

Hardware

Next it is time to connect the particulate matter sensor. The physical layout of the PM sensor connections are shown in Figure 13. The pin descriptions can be found on Table 17.

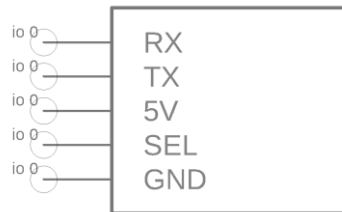


Figure 13 - Shinyei Particulate Matter Sensor Layout

Table 17 - Shinyei PM Sensor Pin Descriptions [17]

PIN Name	PIN Num.	Type	Description
GND	1	Input	Universal ground for power and signal
SEL	2	Input	Output Mode, Continuous or on Command Response
5V	3	Input	5V power Supply
TX	4	Output	UART (3.3V) data transmitter
RX	5	Input	UART (3.3V) data receiver

The 5V pin is connected to the 5V rail, GND is connected to the universal ground of the system, SEL is connected to ground and TX is connected to the ATmega Pin as seen on Table 18. Note that the RX pin on the Shinyei PM sensor is not connected.

Table 18 - Shinyei PM Sensor Pin Assignments

Shinyei PM Sensor Pins	Arduino Label	Arduino Mega Pin	Atmega 2560 pins (Custom PCB)
TX	RX3	15	63

Software

The particulate matter sensor outputs a serial message of 29 bytes. In order to get all the bytes and separate them into useful information we first read the byte stream and place it in a buffer. The buffer is separated in 29 bytes but much of the information we want to extract from it is encoded in two bytes or more. In order to get the information when there is more than one byte we do the following. We create a variable and assign it to the first byte, then we shift it by 8 bits to the left and last we OR it with the next byte in the buffer. This can be seen in Figure 16 - FONa 808 3G and GPS Module LayoutFigure 14.

```
uint16_t d3 = (uint16_t)Buffer[3] << 8;
d3 |= Buffer[4];
```

Figure 14 - Extracting Two Bytes from Buffer

The message structure is structured in the following way. As seen on

Table 19. The mass concentrations of data D3 – D6 is measured in $\mu\text{g}/\text{m}^3$. D7 – D10 is measured as the occupancy ratio of particles greater than the specified value.

Table 19 - Particulate Matter Sensor Data Structure [17]

Symbol	Data Length	Message Content	Value	Units
STX	1	Start	0x02	
D1	1	Number of Bytes transmitted	29	
D2	1	Command	0x10	
D3	2	Mass Concentration (10 Seconds)	0x00-0x03E8	$\mu\text{g}/\text{m}^3$
D4	2	Mass Concentration (30 Seconds)	0x00-0x03E8	$\mu\text{g}/\text{m}^3$
D5	2	Mass Concentration (60 Seconds)	0x00-0x03E8	$\mu\text{g}/\text{m}^3$
D6	2	Mass Concentration (180 Seconds)	0x00-0x03E8	$\mu\text{g}/\text{m}^3$
D7	2	P0.5 Pulse Ratio Output	0x0 - 0x2710	1/10000
D8	2	P0.7 Pulse Ratio Output	0x0 - 0x2710	1/10000
D9	2	P1.0 Pulse Ratio Output	0x0 - 0x2710	1/10000
D10	2	P2.5 Pulse Ratio Output	0x0 - 0x2713	1/10000
D11	2	Status	-	
D12	1	Software Version	-	
D13	4	Production Number	-	
ETX	1	End of Text	0x03	
D14	1	Checksum	-	
EOT	1	End of Transmission	0x04	

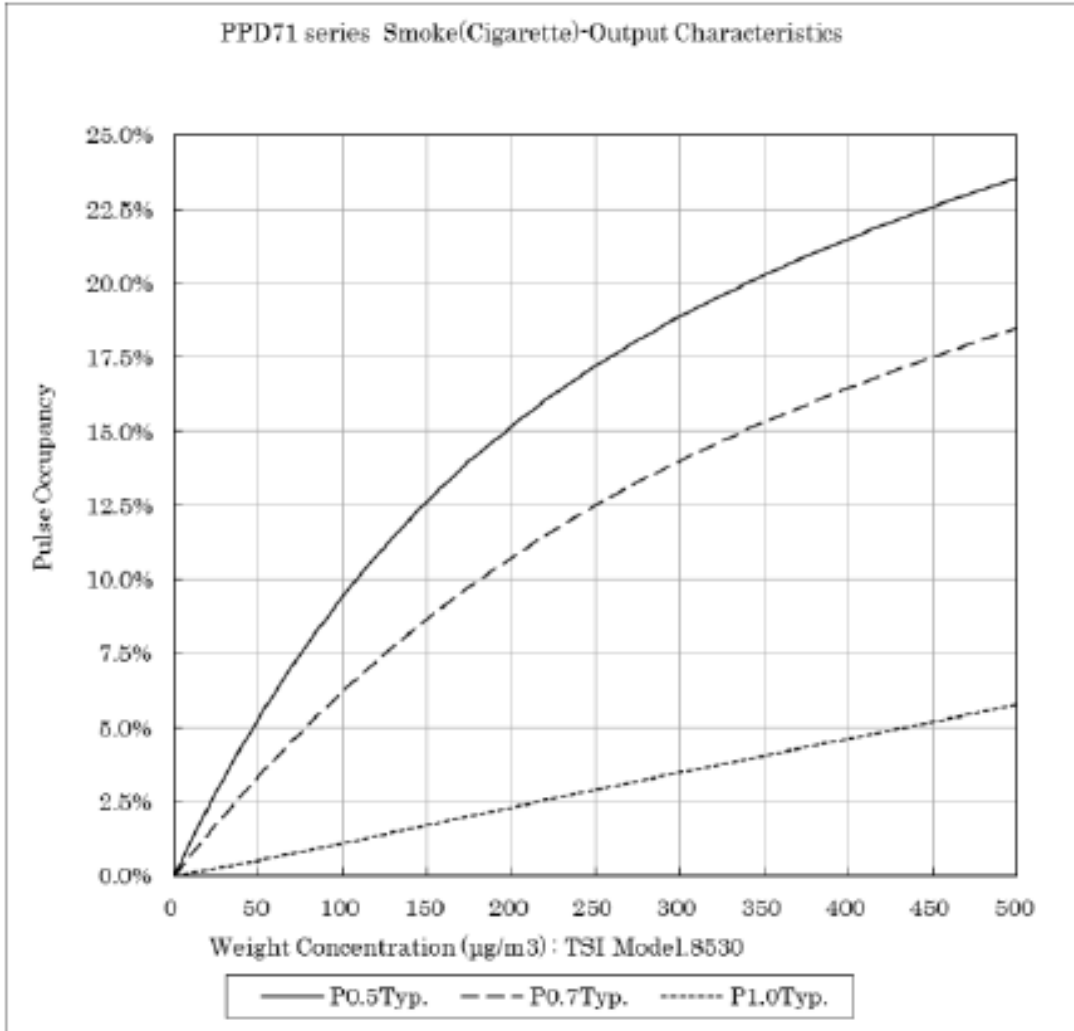


Figure 15 - Pulse Occupancy Ratio vs Weight Concentration [17]

4.3 FONA 808

Hardware

We have connected all of the components we need in order to obtain the air quality data. Now we need to obtain the GPS location and be able to send the data to the online database. For this, we will be connecting the FONA 808 GPS & 3G Module.

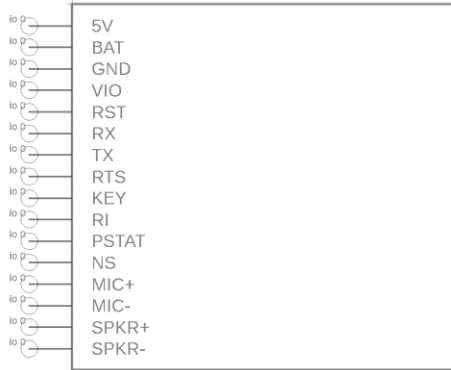


Figure 16 - FONA 808 3G and GPS Module Layout

Table 20 the different pins on the FONA 808 are described. In Table 21 the connections of the module with the microcontroller are defined.

Table 20 - FONA 808 Pin Descriptions

PIN Name	PIN Num.	Type	Description
5V	1*	Input	Power Supply (5V)
BAT	2	Input	
GND	3*	Input	Universal ground for power and signal
VIO	4*	Input	Voltage Input and Output Pin. This pin sets the voltage level for the logic. For our case this pin will be powered to 5V.
RST	5*	Input	Reset pin. For a hard reset toggle this pin to low for 100ms.
RX	6*	Input	UART data receiver
TX	7*	Output	UART data transmitter
RTS	8	Input	Hardware control pin. Controls data transmission between the micro controller and the SIM808 embedded in the FONA 808.
KEY	9*	Input	Power on/off switch. Ground for 2 seconds to turn module on or off. If you wish to leave it on all the time ground it.
RI	10	Output	Ring Indicator. Interrupt pin output from the module. It is high by default and will output a low pulse for 120ms when a call is received.
PSTAT	11	Output	Power status pin. This pin will output a high logic when the module is on and a low logic when the logic is off.
NS	12	Input	Network Status, it pulses to show the current status of the module.
MIC+	13	Input	Microphone input (+)
MIC-	14	Input	Microphone input (-)
SPKR+	15	Output	32 Ohm Speaker output (+)
SPKR-	16	Output	32 Ohm Speaker output (-)

* Connected in system

Table 21 - FONA Module Pin Assignments

FONA 808	Arduino Label	Arduino Mega Pin	Atmega 2560 pins(Custom PCB)
RST	PWM 4	4	1
RX	PWM 2	2	23
TX	PWM 10	10	6

Software

The data that is collected from our system will be sent to a data base server, namely Ubidots. Ubidots is compatible with the FONA 808 module as it features a comprehensible library to communicate with the device [18]. Ubidots is an online platform that provides hosting of data points, intuitive visualizations and provides basic analysis tools.

We modified the *Ubidots FONA Library* by adding two functions, namely `setupGPS` and `getGPS` as seen on Figure 17. We also modified the `UbidotsFONA.h` file by changing the `MAX_VALUES` to 10 so we can send more data during the same connection.

Then we created a file within our code file to communicate with the Ubidots FONA Library, this code can be seen in Section *Ubidots.cpp*.

```

bool Ubidots::setupGPS () {
  // fonaSerial = fonaSS;
  while(!Serial);
  Serial.println("Setting up GPS");
  GPSCoordinates coord;

  if (!adafruitFona.begin(*fonaSerial)) {
    Serial.println(F("FONA not found"));
    while (1);
  }
  //Enable GPS
  adafruitFona.enableGPS(true);
  Setup = true;
  Serial.println(Setup);
  return true;
}

GPSCoordinates Ubidots::getGPS () {
  int i =0;
  GPSCoordinates coord;
  boolean gps_success = adafruitFona.getGPS(&coord.latitude,
&coord.longitude, &coord.speed_kph, &coord.heading,
&coord.altitude);

```

```

    if (gps_success) {
        Serial.println(coord.latitude);
        return coord;
    }
    coord.latitude = 200.123456;
    coord.longitude= -200.654321;
    return coord;
}

```

Figure 17 - UbidotsFONA Modifications for GPS Acquisition

4.4 Atmega 2560

Hardware

In order to program the Atmega 2560 we used an external Arduino as an In-Circuit Serial Programmer (ISP). For this specific task, we allotted six pins to be used as seen on Table 22 - Programming Pins Atmega2560. In addition to leaving this pins connected to female headers to connect the programmer we need to connect a 16Mhz Oscillator between pins XTAL1 and XTAL2 of the Atmega2560 and with a 22pF capacitor between XTAL1 and GND and another 22pF capacitor between XTAL2 and GND as seen on Figure 18.

Table 22 - Programming Pins Atmega2560

Name	Atmega2560	Arduino Uno
Reset	30	10
MOSI	21	11
MISO	22	12
SCK	20	13
GND	GND	GND
5V	VCC	VCC

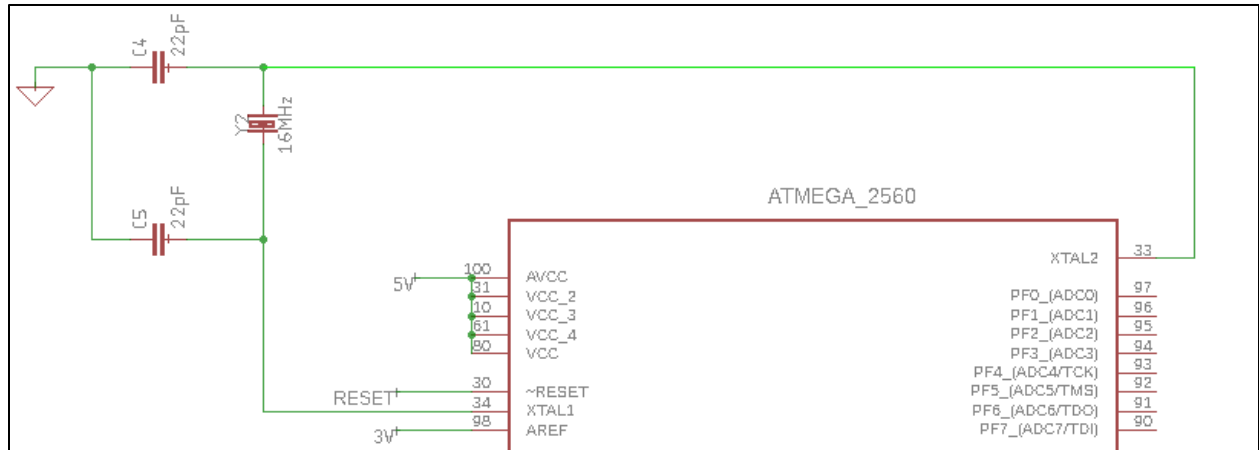


Figure 18 - Oscillator Connection to Atmega2560

Software

The code has been designed to collect the data of the different sensors and GPS and store them in multiple arrays. The length of these arrays is limited by the space available in the microcontroller's memory. For testing purposes, we set the size of the arrays to a variable `LOOPS` and set it equal to five. After the five pieces of data have been collected, the Ubidots function to send the data is called `LOOPS` times.

In order to ease the communication within the system we created data structures specific to each sensor, so that it would be easier to access them.

Table 23 - Data Structures for data acquired

GPS Coordinates	PM Sensor	SPEC Sesnsors
<pre>typedef struct GPSCoordinates{ float latitude; float longitude; float speed_kph; float heading; float altitude; };</pre>	<pre>typedef struct pmSensorResults{ uint8_t stx; uint8_t d1; uint8_t d2; uint8_t d3; uint16_t d4; uint16_t d5; uint16_t d6; uint16_t d7; uint16_t d8; uint16_t d9; uint16_t d10; uint16_t d11; uint16_t d12; uint32_t d13; uint8_t etx; uint8_t d14; uint8_t eot; float pm05_occupancy; float pm07_occupancy; float pm10_occupancy; float pm25_occupancy; } ;</pre>	<pre>typedef struct SpecSensorsResults{ float CO; float NO2; float SO2; float H2S; float O3; float TEMP; };</pre>

4.5 Solar Power and Battery

We worked closely with Kayleah Griffen to integrate the solar power system to our overall design. For this, we created connections on the PCB board to connect measure and control the power system. The power system includes an algorithm that optimizes the battery charging, namely Maximum Power Point Tracking. See Appendix A.

4.6 Final Hardware Layout

The last step in the hardware design process was to create a PCB board. For this, we used Eagle Autocad Software to create the schematic and then translate it into a PCB. The schematic can be seen in Figure 22 and the board can be seen in Figure 20.

We used a set of two linear voltage regulators to supply the needed voltage to all of the components. The first linear regulator is fed by the battery. It has an output voltage

of 5V and supplies power to the Atmega 2560 microprocessor, the FONA 808 and the PM Sensor. The 5V linear regulator is also connected to the 3V linear regulator which supplies power to all of the spec sensors and op amps needed in the sensors operations.

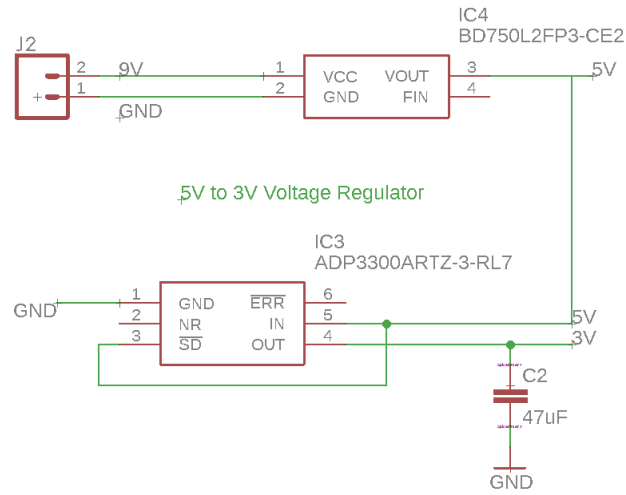


Figure 19 - Voltage Regulators in PCB Design

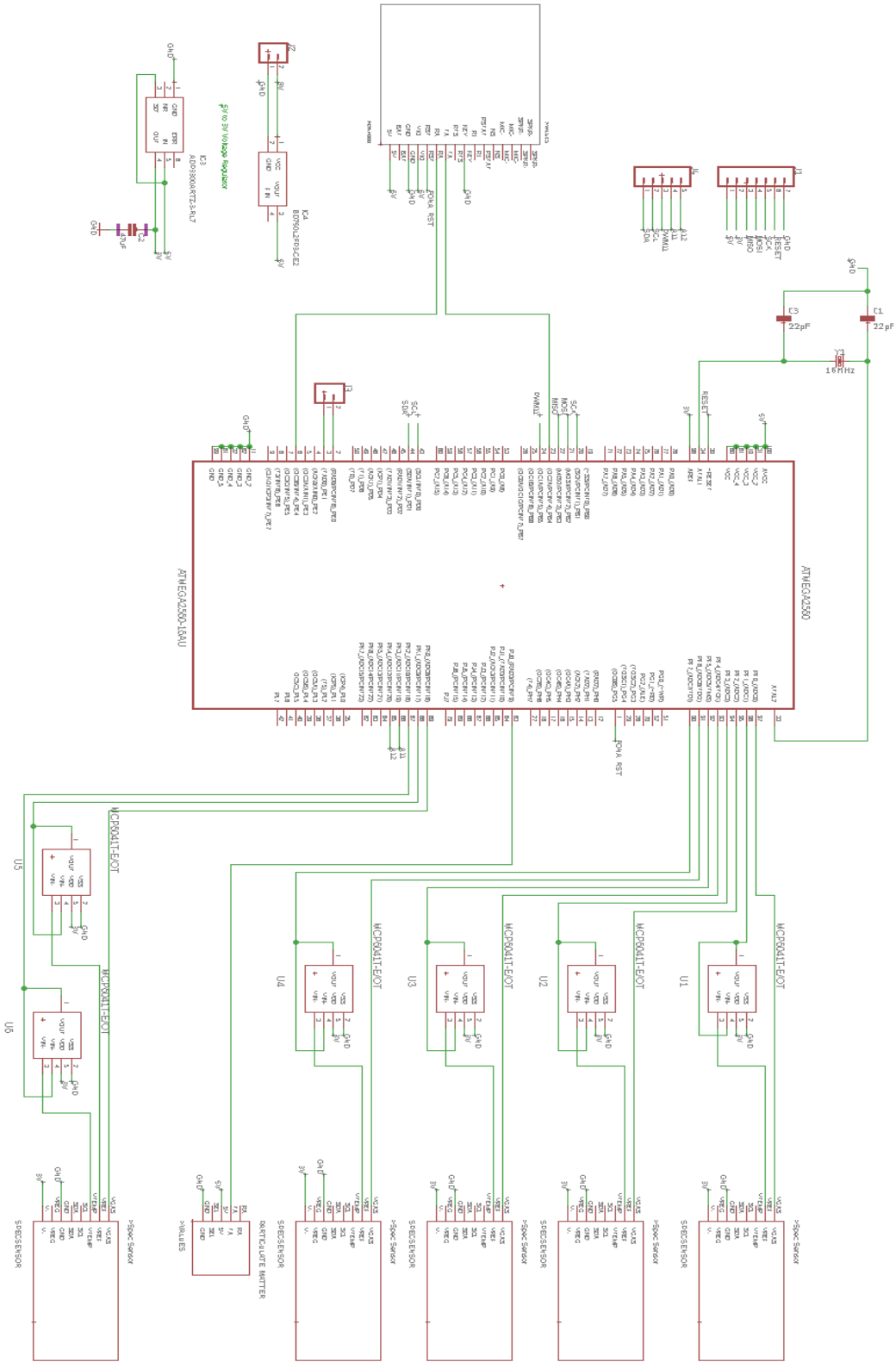


Figure 20 - Overall Schematic without Solar Power and Battery Design

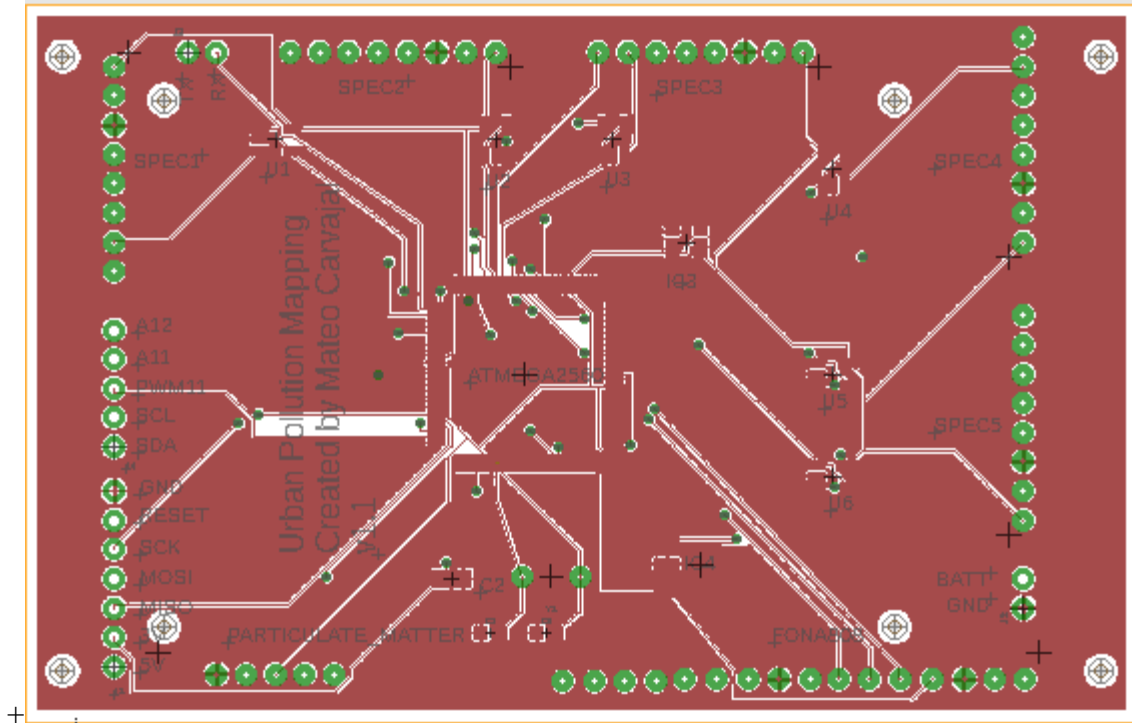


Figure 21 - Top of PCB

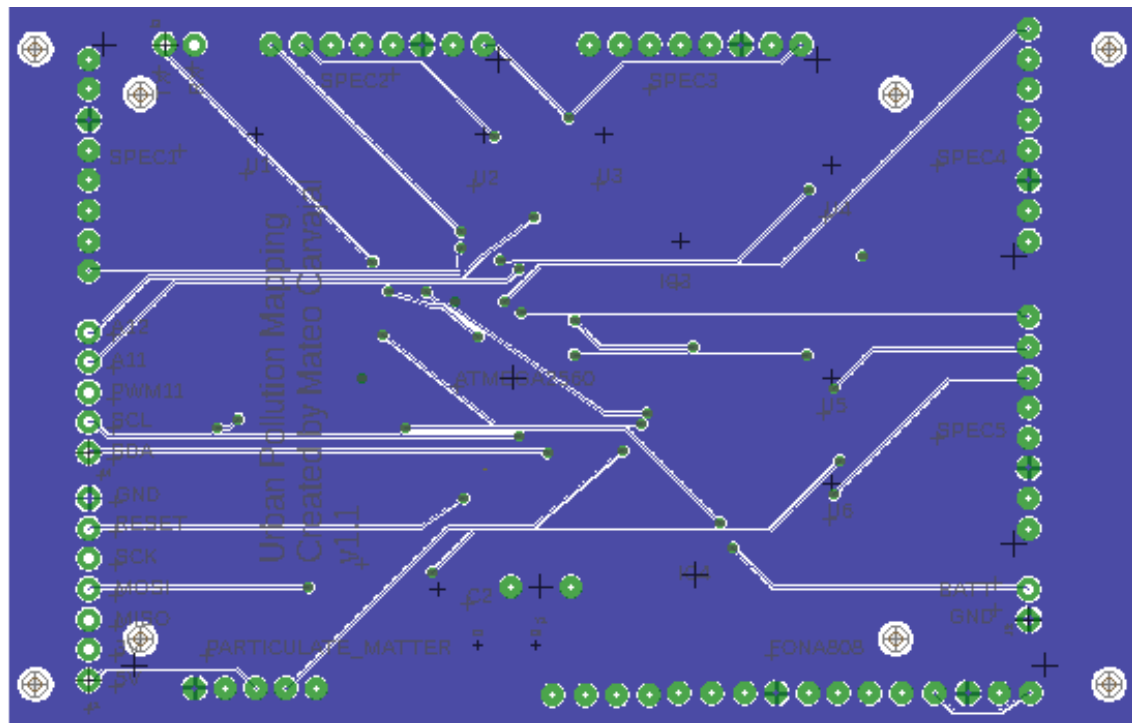


Figure 22 – Bottom of PCB

5. Results

Throughout our project, we were able to test the functionality of the different components. In this section, we describe the challenges and results we faced while trying to obtain the data.

Our main goal of developing a prototype with extensive functionalities has been achieved. The prototype sits on a custom PCB able to measure five different gases, monitor particulate matter, record the GPS location, transmit the data to an online server and power itself using solar power.

First off, we tested our temperature sensor response. Having the temperature on hand is extremely important while running data analysis on the different gases since the SPEC sensors require different adjustments with different temperatures. In Figure 23 the temperature remains constant just under 25°C until second 48 where we grab the sensor with the hand to increase the temperature. Then at second 65, we let go of the sensor. As you can see the sensor responds appropriately to a sudden change in the environment and takes a longer a period of time to cool down.

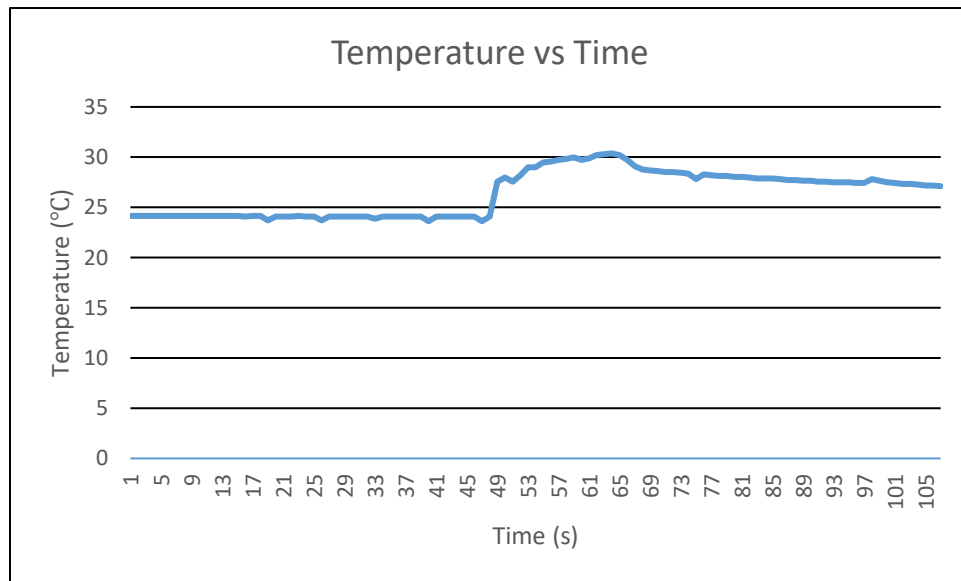


Figure 23 - Temperature Sensor Results

We also tested the connection of the PM sensor to verify we were getting the correct data sent by the PM module. For this we compared the values we expected (

Table 19) with the experimental results (Figure 24). All of the fixed values match.

D1	Number of Bytes Transmitted:	29
D2	Command(Fixed Value):	16
D3	Mass Concentration 10s:	4
D4	Mass Concentration 30s:	1
D5	Mass Concentration 60s:	1
D6	Mass Concentration 180s:	0
D7	0.5um Pulse Ratio Output:	65510
D8	0.7um Pulse Ratio Output:	0
D9	1.0um Pulse Ratio Output:	0
D10	2.5um Pulse Ratio Output:	0
D11	Status:	4096
D12	Software Version:	15
D13	Production Number:	383
ETX:		3
D14	Checksum:	197
EOT:		4
PM 0.5	Occupancy:	6.00

Figure 24 - Results from PM Sensor Message

Next, we tested the GPS coordinates response. The results obtained can be seen in Figure 25. Where “42.268302” is the latitude and “-71.804400” is the longitude. This coordinates match precisely to where the device was located for the measurement.

```
----> AT+CGNSINF
<---- +CGNSINF: 1,1,20180426043645.000,42.268302,-71.804400
```

Figure 25 - GPS Response

```
FONA/3.0|POST|A1E-e410VDZ0TBihwsxssuJxPltjnjdBlL|FONA=>CO:
65.98,NO2: 44.38,SO2: 0.00,H2S: 56.22,O3: 11.17,Temp:
20.88,PM2.5: 0.00,PM0.5: 0.00,Coordinates:
1.00$lat=195.200$lng= 0.570,Batt Voltage: 32.76|end

Response of FONA:

OK

OK
```

Figure 26 - HTTP Post Command and FONA Response

After having implemented each individual component, we were able to join all the sensors to operate simultaneously and to send the data to the database via the wireless transmitter. An example of the results can be seen in Figure 27.

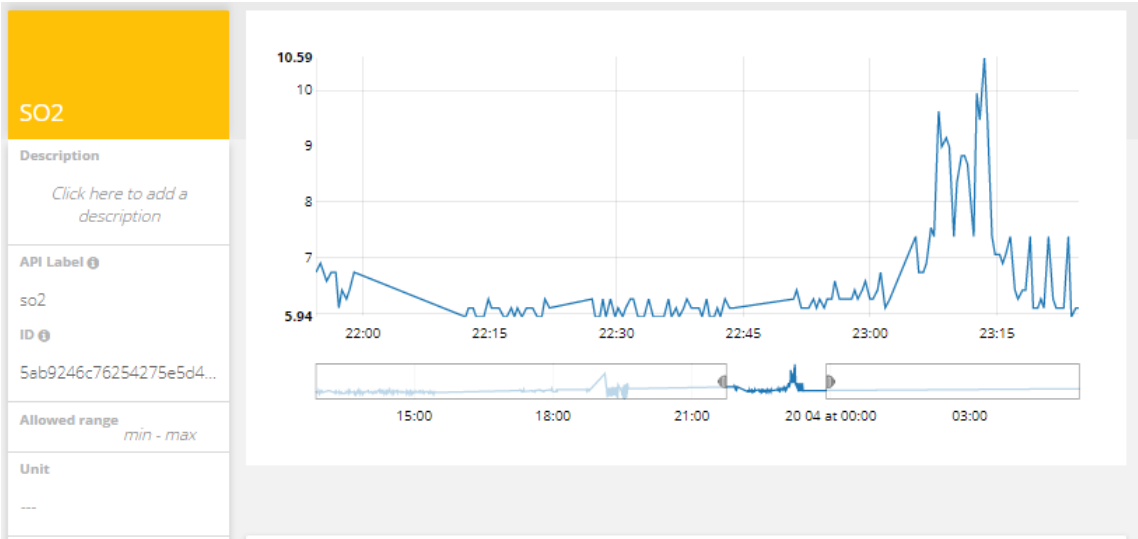


Figure 27 – Sulfur Dioxide Ubidots Results

Throughout our project, we also sought to design tests to verify the different sensors and the accuracy of the measurements. Unfortunately, testing the gas sensors was extremely challenging. While we were able to verify that the sensors were working electrically and sending data, we we’re not able to perform accurate measurements of specific gas concentrations. First of all, the gases measured by the sensors are all toxic

and acquiring test samples was difficult. Also, the SPEC sensors have a prolonged reaction time of ~2min. Controlling the space around the sensors was extremely challenging. In addition to this we had no enclosed facilities designed to test gas concentrations, so the experiments we conducted to measure specific gases returned no valuable data points.

The physical layout of our finalized prototype can be seen in Figure 28. The system pictured has been able to record and send the data to the database successfully.

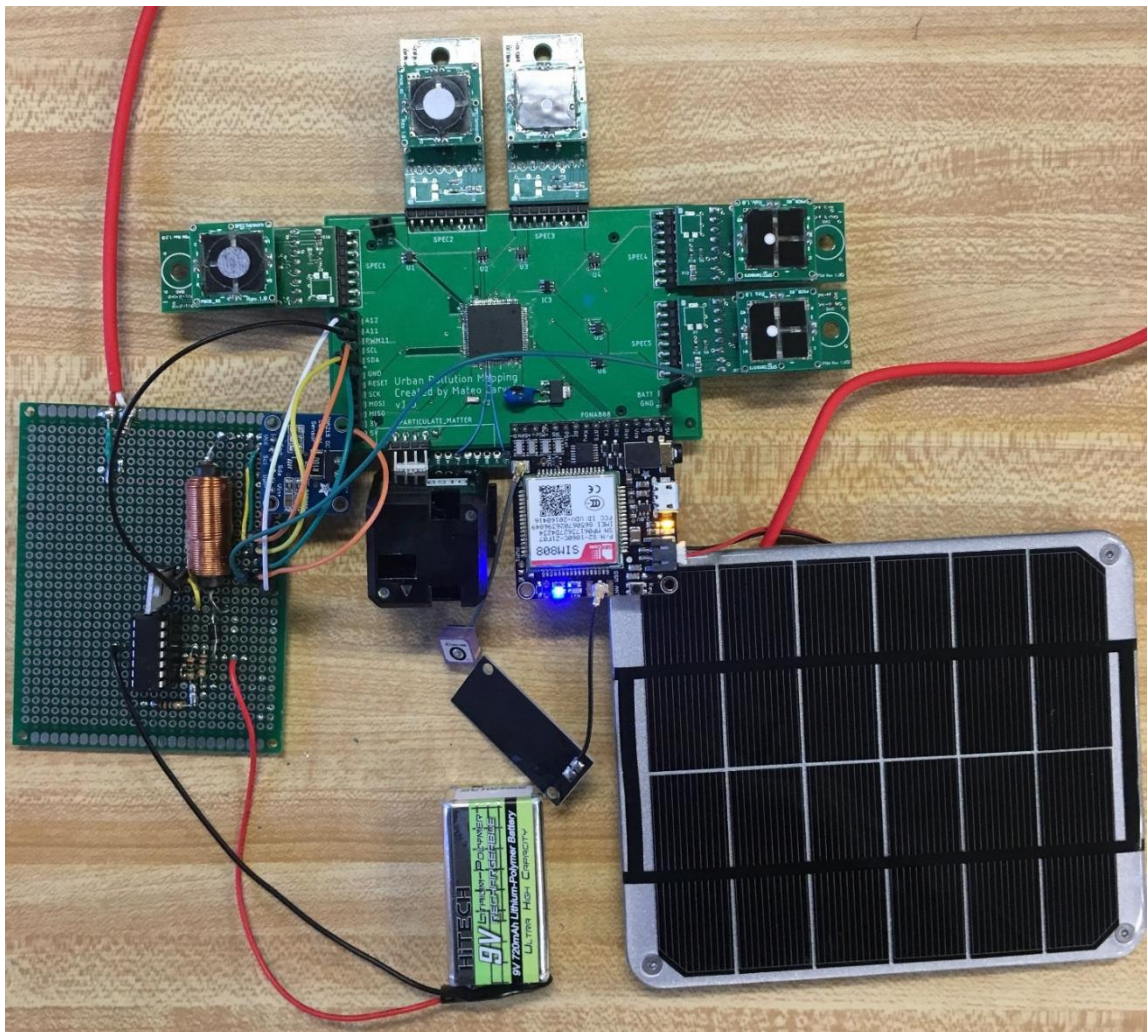


Figure 28 – Final Prototype of our solar powered pollution measurement system

6. Conclusion and Recommendations

Air pollution in urban environments represents a grave risk to human health and well-being. Collecting air pollution data has the potential to become an important tool in an urban planner's hands to make better and effective changes to reduce the harmful gases. It can also have many uses if the data is available to the public, especially in creating awareness and fueling advocacy.

Regarding this project, most importantly, we successfully developed a prototype to monitor the six main air pollutants that threaten health in our cities. The prototype calculates the levels of the pollutants and wirelessly transmits the data to an online database. In addition to this we have created a self-sufficient power system that powers itself from sun light and charges a battery when there is adequate lighting. When the photovoltaic cells are not active, the battery supplies power to the system.

The objective of creating a prototype that would monitor and report air quality to an online database while harvesting its energy from its surrounding has been achieved. Nevertheless, considerable more work needs to occur in order to create a comprehensive device that can reliably provide air quality data over long periods. We also recommend conducting a detailed analysis of the SPEC sensors. Unfortunately, the available data from and reviews of the SPEC sensors are very limited. However, we have been told, informally, by experts in the field that the sensors can be sensitive to humidity. If this system were to be used on a large scale throughout cities, an investigation on the accuracy of the SPEC sensors over a variety of meteorological conditions must be made to ensure the data gathered is accurate under all conditions.

Air quality is not uniform and can change rapidly due to many factors, we recommend that the system be equipped with machine learning and artificial intelligence algorithms to better predict the levels of pollutants and create more comprehensive pollutant maps.

7. Bibliography

- [1] World Health Organization, "Ambient air pollution: A global assessment of exposure and burden of disease," 2016.
- [2] M. Brauer, "Ambient Air Pollution Exposure Estimation for the Global Burden of Disease 2013," *Environmental Science & Technology*, pp. 79-88, 2015.
- [3] OECD, "OECD Environmental Outlook to 2050: The Consequences of Inaction.," Publishing, Paris, 2012.
- [4] EPA, "Latest Findings on National Air Quality," United States Environmental Protection Agency, 2008.
- [5] World Health Organization, "Health Aspects of Air Pollution with Particulate Matter, Ozone and Nitrogen Dioxide," Bonn, Germany, 2003.
- [6] United States Department of Labor (OSHA), "Hydrogen Sulfide," [Online]. Available: <https://www.osha.gov/SLTC/hydrogensulfide/hazards.html>. [Accessed 2018].
- [7] Luft Hamburg , "Luftmessstation Hamburg-Stresemannstraße," [Online]. Available: <http://luft.hamburg.de/messstationen-liste/4244982/17sm-stresemannstrasse.html>. [Accessed April 2018].
- [8] A. Carvajal, *Hamburg Air Quality Monitoring Station*, Hamburg, 2018.
- [9] SPEC Sensors, SPEC Sensor Operation Overview, May 2016.
- [10] SPEC Sensors, "Ultra-Low Power Analog Sensor Module for Carbon Monoxide" ULPSM-CO 968-001 Datasheet, October 2016.
- [11] SPEC Sensors, "Ultra-Low Power Analog Sensor Module for Nitrogen Dioxide" ULPSM-NO2 968-047 Datasheet, August 2017.
- [12] SPEC Sensors, "Ultra-Low Power Analog Sensor Module for Sulfur Dioxide" ULPSM-SO2 968-006 Datasheet, October 2016.
- [13] SPEC Sensors, "Ultra-Low Power Analog Sensor Module for Hydrogen Sulfide" ULPSM-H2S 968-003 Datasheet, October 2016.
- [14] SPEC Sensors, "Ultra-Low Power Analog Sensor Module for Ozone" ULPSM-03 968-046 Datasheet, August 2017.

- [15] Shinyei Technology, "PPD 71 Particle Sensor Unit," [Online]. Available: http://www.shinyei.co.jp/stc/eng/optical/main_ppd71.html. [Accessed January 2018].
- [16] Novatel, "Chapter 3 GNSS Satellite Systems," [Online]. Available: <https://www.novatel.com/an-introduction-to-gnss/chapter-3-satellite-systems/beidou/>. [Accessed March 2018].
- [17] Shinyei Technology CO., "Particulate Matter Sensor" PPD71 Datasheet, August, 2017.
- [18] Ubidots, "Ubidots FONA Library," 2016. [Online]. Available: <https://github.com/ubidots/Ubidots-FONA>. [Accessed March 2018].
- [19] N. Mohan, T. Undeland and W. P. Robbins, Power electronics: Converters, applications, and design (3rd ed.), Hoboken, NJ: John Wiley & Sons, 2003.
- [20] N. Notman, "Chemistry World," 12 January 2017. [Online]. Available: <https://www.chemistryworld.com/feature/urban-air-pollution/2500224.article>.
- [21] M. L. Melamed, T. Zhu and L. Jalkanen, "Urban Air Pollution: a new look to an old problem," *IGBP's Global Change Magazine*, 2013.
- [22] T. Zhu, M. L. Melamed, D. Parrish, M. Gauss, L. Gallardo Klenner, M. Lawrence, A. Konare and C. Liousse, "Impacts of Megacities on Air Pollution and Climate," 2012.
- [23] EPA, "Basic Information about NO₂," [Online]. Available: <https://www.epa.gov/no2-pollution/basic-information-about-no2#Effects>.
- [24] Diodes Incorporated, 1N5817 - 1N5819 1.0A Schottky Barrier Rectifier [Data Sheet], April, 2018.
- [25] GN Batteries and Electronics, Inc, RLI-9720 Li-Ion Polymer Battery Pack [Data Sheet], 2011.
- [26] International Rectifier, IRL2703 HEXFET Power MOSFET [Data Sheet].
- [27] Microchip, MCP6041/2/3/4 Op Amp Datasheet, 2013.
- [28] Texas Instruments, Zero Drift, Bi-Directional Current/Power Monitor with I2C Interface [Data Sheet], 2011.
- [29] Voltaic Systems, 2W 6V 112x136 mm Solar Panel [Data Sheet], 2017.
- [30] Voltaic Systems, "Small Solar Panels," [Online]. Available: <https://www.voltaicsystems.com/solar-panels>. [Accessed 24 04 2018].

- [31] N. Femia, G. Petrone and M. Vitelli, Power electronics and control techniques for maximum energy harvesting in photovoltaic systems, CRC Press, 2013.
- [32] Y. Mahmoud, W. Ziao and H. H. Zeineldin, "A parameterization approach for enhancing PV model accuracy," *IEEE Transactions on Industrial Electronics*, 2013.

8. Appendix

Appendix A: Solar Power and Battery

Solar Power Design

This chapter of the report, written by Kayleah Griffen, provides auxiliary material developed by Kayleah Griffen to do more in depth ECE work for the fulfillment of her second degree. The work presented in this chapter complements the MQP of Mateo Carvajal: Mapping Urban Pollution. Mateo Carvajal's MQP can be separately referenced for additional context on urban pollution. The purpose of the work described in this chapter is to provide the power system for the urban pollution mapping system. By using solar energy charging the urban pollution mapping system would be able to be self-sufficient in terms of power and therefore operate independently without service for longer periods of time. Based on the power consumption of the system and the microcontroller selected, a solar panel, battery, and a boost converter were chosen for the system. The power generation system implemented used a maximum power point tracking algorithm in order for it to harvest the most energy from the solar panel to maximize the use of the solar panel. The components selected in this project were the solar panel, battery, inductor, MOSFET, diode, as well as the voltage and current sensing subsystems. The Practical Model of the solar panel was modeled in MATLAB and the entire charging system was modeled in Simulink prior to actually building the system. Simulation allowed for more informed decisions about the sizes of certain components as well as to better understand the system behavior. After the system was designed, simulated and modified it was constructed and tested.

Solar Panel and Battery Selection

The first components selected that served as a baseline for the solar charging system were the battery and the solar panel. The power consumption of the system was estimated in order to make the correct decision on what power ratings for the battery and the solar panel were needed. The power consumption estimates for the urban pollution mapping system components are shown in Table 24.

Table 24 - Power Consumption Analysis

Part Name	Part Number	Power	Units
Microcontroller	Arduino Mega 2560	500	uW
CO Spec Sensor	110-102	50	uW
NO2	110-501	50	uW
H2S	110-303	50	uW
SO2	110-601	50	uW
O3	110-407	50	uW
PM	PPD71	100000	uW
GPS	Adafruit Ultimate GPS	66000	uW

If the entire urban pollution mapping system was on, it would consume 167 milliWatts. Based on the known power consumption, the battery and solar panel could be selected. The main criteria in selecting a battery was the acceptable charging current, the voltage, the capacity of the battery, and the physical size of the battery. In order to keep a battery safe, the battery must be able to accept the full range of the solar panel currents. This is because at the maximum power point voltage of the solar panel is controlled but not current. If the maximum power point of the solar panel occurs at a current that is higher than what the battery could accept, then the current would need to be limited. This would defeat the purpose of maximum power point tracking, therefore a battery was selected that could accept the full range of currents of the solar panel. The acceptable voltage range for the raw power input pin of the microcontroller limited the battery voltages that were possible, this was 7-12 Volts. For the solar panel the main criteria were the rated power and the size. A solar panel was generously donated from Voltaic Systems, so this narrowed the potential options for panels to 1W, 2W, 3.5W, 6W or 9W rated power, panels with an open circuit voltage above 12V were not considered. The solar panel options are summarized in Table 25 (Voltaic Systems).

Table 25 - Solar Panel Comparison (Voltaic Systems)

Panel	1	2	3.5	6	9
Open Circuit Voltage (V)	7.7	7.7	7.7	7.7	7.7
Peak Current (mA)	180	340	550	930	1,420
Peak Power (W)	1.2	2.2	3.5	6	9.2
Size	3.5" x 4.4"	5.4" x 4.4"	8.3" x 4.4"	8.3" x 4.4"	8.7" x 10.1"

Based on these solar panel options, research was conducted to determine what battery could work with the solar panels. The peak current of the solar panel severely limited the batteries that could be selected because most batteries charge at smaller currents than the peak currents seen in the solar panel options. For this reason the GN Batteries & Electronics Inc Lithium Ion Polymer Battery Pack was selected for its ability to accept the peak current. This battery had a nominal voltage of 7.4 Volts, a charge voltage of 8.4 Volts, and a charge current of 370 mA up to 740 mA (for a rapid charge), and a capacity of 740mAh (GN Batteries & Electronics, Inc, 2011). With a capacity of 740mAh the battery could last 4.5 hours if all of the systems of the battery were on at the same time. All of the sensors do not take readings all of the time and due to this the battery life was expected to last much longer than 4.5 hours. Now that the battery was selected, the final selection for the solar panel could be made. The 2W solar panel most closely aligned with the charging current of the battery, additionally it was small in size which was desired. In peak conditions the 2W solar panel could charge the battery fully in approximately 2 hours. Therefor the battery and the solar panel selection was made by best matching the power demands of the system, the microcontroller voltage, and the sizing considerations. The selection of the solar panel and the battery were intertwined with each other as decisions about the solar panel impacted the battery and vice versa.

Maximum Power Point Tracking Using Boost DC/ DC Converter

A dynamical optimizator is defined as a mechanism that accounts for the time varying maximum power point of solar panels and controls the solar panel in order for it to operate at its maximum power point; most often this is implemented with a DC/DC converter with a controllable duty cycle (Femia, Petrone, Spagnuolo, & Vitelli, 2013). Maximum power point tracking was an important part of this project because with a small 2W solar panel, fixing the voltage operating point could severely limit the power output of the solar panel. The solar panel characteristics are heavily influenced by the temperature and the irradiance, which is further described in the Section "Implementation: Practical Model of the Solar Panel". However in order to give an idea for how temperature and irradiance affect the power output of the solar panel, the Voltage vs Power curve is shown in Figure 29. This plot was generated in MATLAB.

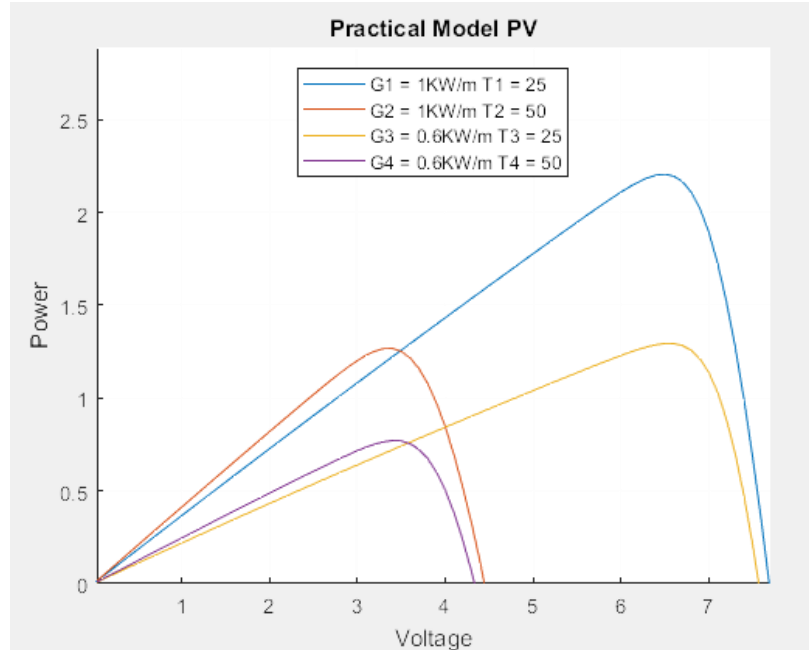


Figure 29 - Voltage vs Power Curve for 2W Solar Panel

By inspecting the graph, it is clear that the irradiance and temperature affect the power curve for the panel. As these conditions vary throughout the day it is important that the solar charging system be adaptable to the varying conditions. The way a system is able to adapt is through the dynamical optimizer, which by changing the duty cycle changes the voltage that the solar panel operates at in order for the panel to operate at its maximum power in any condition.

The dynamical optimizers selected for this project was a DC/DC converter with a Boost Converter topology. This topology was used because the battery voltage would always be higher than the solar panel voltage, therefore the voltage of the solar would always need to be “boosted” to attain the battery voltage. A basic schematic for a standard layout of a DC/DC boost converter is shown in the figure below, as this was used to develop the DC/DC boost converter that was actually used with the solar panel. First the basic schematic of a DC/DC boost converter will be described, then the way that the values were chosen and finally how this model was adapted to do the maximum power point tracking will be explained.

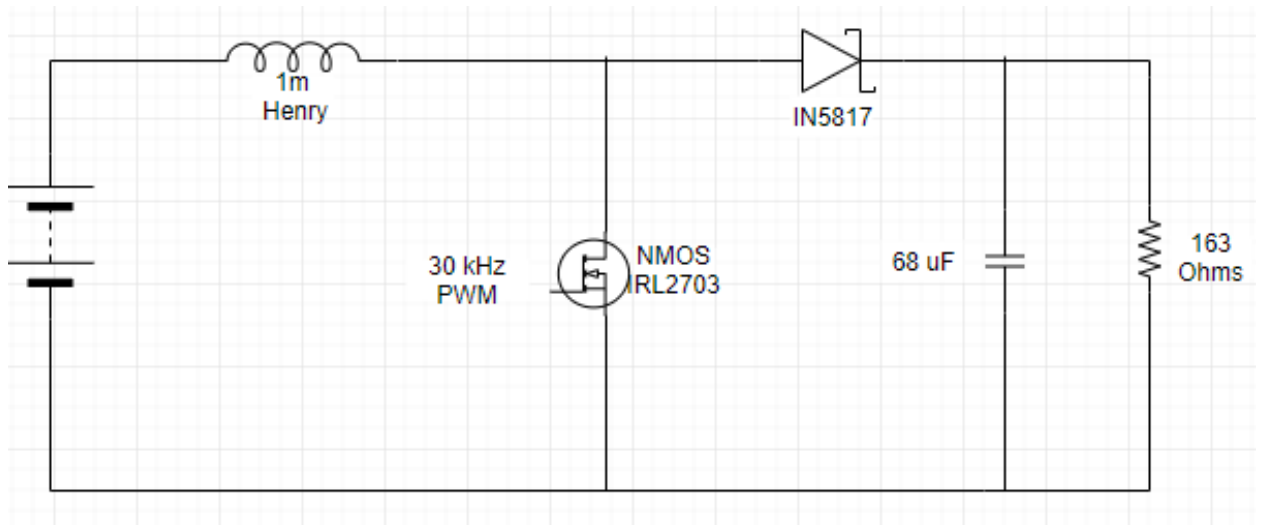


Figure 30 - Basic Layout of DC/DC Boost Converter

The DC/DC boost converter was designed assuming continuous conduction mode, meaning that current is always flowing through the inductor (Mohan, Undeland, & Robbins, 2003). When the MOSFET gate is open current flows through the charged inductor through the diode to the load, with the inductor and the supply providing the power. When the MOSFET gate is closed then the diode becomes reverse biased and does not allow current through, during this time the inductor is charging (Mohan, Undeland, & Robbins, 2003). The frequency for the switching was determined to be 30kHz. Based on this frequency as well as the known input voltage, 0 - 7.7 Volts (based on the solar panel voltage range) and output Voltage range 7.4 Volts (based on the battery voltage) a duty cycle range, capacitance and inductance could be determined. It is noted that because this is a boost topology the input voltage cannot go above 7.4 Volts for the output to be 7.4 Volts (if the input did go above then a buck boost converter would be needed).

The duty is related to the voltage by the following equation:

$$\frac{V_o}{V_d} = \frac{T_s}{t_{off}} = \frac{1}{1-D} \quad [19]$$

Where V_o = Output voltage, V_d = Input Voltage, T_s = Switching time (inverse of PWM frequency), t_{off} = time off in a T_s interval, D = duty cycle

Solving for the duty cycle:

$$D = 1 - \frac{V_d}{V_o}$$

This equation reveals that for a fixed output voltage to be attained with a variable input voltage, when the input voltage is at a low the duty cycle is at a high and when the input voltage is at a high the duty cycle is at a low.

Additionally the worse case capacitance could be solved for, the formula for capacitance is:

$$C = \frac{I_o D T_s}{\Delta V_o} \quad [19]$$

Where I_o = Output Current, D = Duty Cycle, T_s = Switching time, and V_o = Voltage Ripple

To solve this equation for the largest capacitor needed, the I_o was set to the maximum output current which was the peak power input current, 340mA, the D was set to the duty cycle at the peak power, which was 0.12, the T_s was the inverse of the 30kHz switching frequency and the voltage ripple was 10% of the maximum voltage, 0.74 Volts. Solving this for the capacitor size, a 1.87 uF value was found. Next the inductor value could be extracted, in this circuit the inductor value is most important to a proper design. The formula to find the inductor is:

$$L = \frac{T_s V_o D (1-D)}{2 * I_{LB}} \quad [19]$$

Where T_s = Switching time, V_o = Output Voltage, D = Duty Cycle, I_{LB} = Average input current

To solve this equation for the inductor needed, again the peak parameters were used. The switching time was the inverse of 30kHz again, the V_o was the peak power voltage output, 6.5V, the duty cycle was the peak power duty cycle, 0.12, and the I_{LB} was the average current which was half of the peak power current, or 170 mA. Solving this for the inductor size, a 67.2uH value was found.

Next, the values for the inductor and the capacitor were modeled in Simulink, and it was found that increasing the size of the inductor by 2 orders of magnitude significantly smoothed the output PV characteristic for changing duty cycles. Based on this observation and based on readily available supplies, the chosen capacitance was 68uF and the inductance was 1mH. For testing purposes the resistor used was a power resistor that was 163 Ohms, which is why these values are presented in Figure 31. The result of increasing the magnitude of the inductor and capacitor are shown in Figure 31 in the Power vs Duty Cycle curves. To create these figures everything was held constant in the DC to DC converters except the inductor and capacitor values were scaled up.

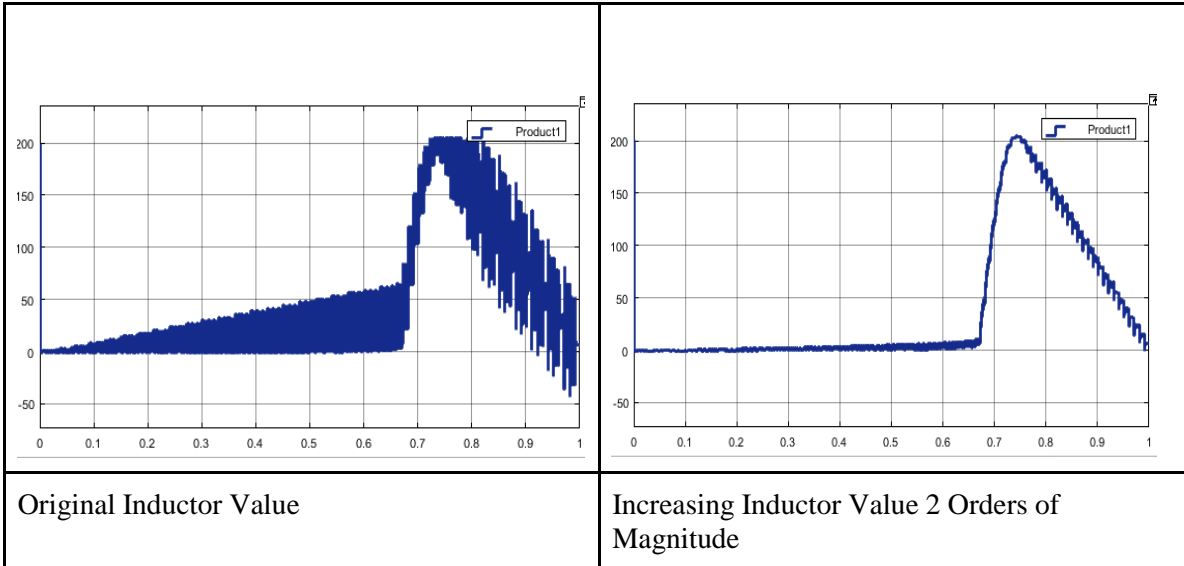


Figure 31 - Inductor Analysis

Now that the component sizing for the DC/DC Boost Converter had been found, it was adapted for the solar panel use. The topology of the boost converter that was designed is shown in Figure 56, the main components are the solar panel, the inductor, the MOSFET, the diode and the battery.

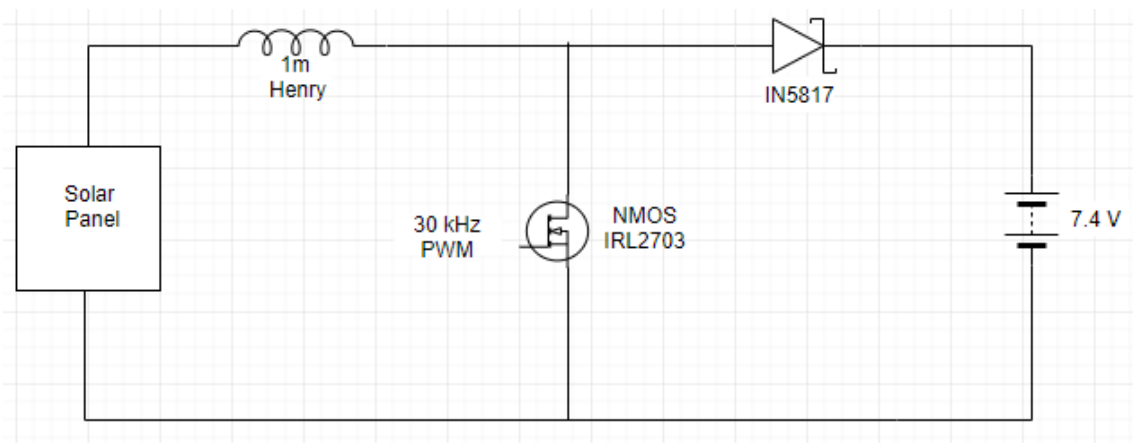


Figure 32 - Solar Charging Boost Converter Topology

In this real implementation the voltage source was replaced for the solar panel, the resistor and capacitor was replaced for a 7.4 Volt Battery, and the last things to select were the MOSFET and the diode that were able to meet the demands of the circuit. Because up to 340mA and 2.2 Watts could flow through the diode, a diode which was rated for those conditions needed to be used. The IN817 diode is rated for a current up to 1A and voltage up to 20V what it is reverse biased; additionally this diode is typically used in switching power supplies and has a low forward voltage drop (Diodes Incorporated, ND). For the MOSFET important considerations were that the drain to

source voltage was small and that the gate be able to be triggered by a 3.3 Volt wave, this was satisfied by the IRL2703 N-MOS (International Rectifier, ND).

In summary, maximum power point tracking is driven by the use of DC/DC converters which act as dynamical optimizers because of their ability to change the operating point of a solar panel through adjusting the duty cycle on the PWM pin. The parts selected to be used for the DC/DC converter were the inductor, diode and the MOSFET.

Sensing Solar Panel Voltage, Current, Power

In order to accomplish maximum power point tracking, the voltage and current of the solar panel must to be monitored in order to interpret the power. In this way previous values for the power of a solar panel can be compared to power values that are the result of changing the duty cycle. This comparison will yield whether an appropriate change in the duty cycle has been made. To monitor the voltage, current and power, the INA219 High Side Current Sensor Breakout sold by Adafruit was selected. The benefits of choosing this specific breakout board was that it had configurable internal gain which allowed for measurements up to a max current of 400mA with 0.1mA precision and voltage up to 32V (Texas Instruments, 2011). This breakout board communicated with the Arduino via I2C and included a library that could be downloaded so that simple function calls could return the current, voltage and power.

Sensing Battery Voltage

The battery characteristic was well matched with the solar panel in that the maximum current that the solar panel could provide would be acceptable by the battery. However in order to monitor whether the battery was charged, in an acceptable range, or had discharged too much the battery voltage needed to be monitored. The battery voltage was monitored with a simple op-amp configured as a voltage follower preceded by a voltage divider, shown in the figure below.

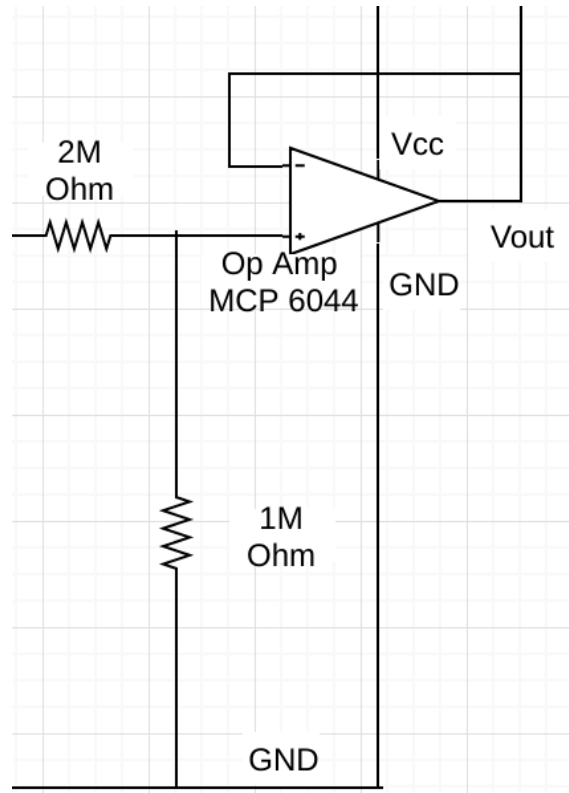


Figure 33 - Voltage Follower and Voltage Divider Circuit

The basic idea of a voltage follower circuit is that there is an op amp with a negative feedback. The voltage at the positive input is the voltage that will be replicated on the output. The benefit of the voltage follower circuit is the high input impedance of the op-amp inhibits current flow through the op amp but preserves the voltage. This is beneficial because then the voltage measurement is not depleting the power. A 2 Mega Ohm and 1 Mega Ohm resistor was used in order for the output voltage to be one third of the input voltage. This was necessary because of the setup of the reference voltage the analog input pins on the microcontroller could only read a voltage between 0 and 3V and the Vout was connected to an analog input pin. The battery voltage could go up to 8.4 Volts so the voltage divider circuit ensured that the output voltage would be at most 2.8V. The op amp selected to do this was the MCP6044 rail to rail op amp, the only requirements were that it needed the Vcc and GND supplied (Microchip, ND).

Overall Schematic and Control Algorithm of Maximum Power Point System

All of the components of the solar charging system are combined in the figure below.

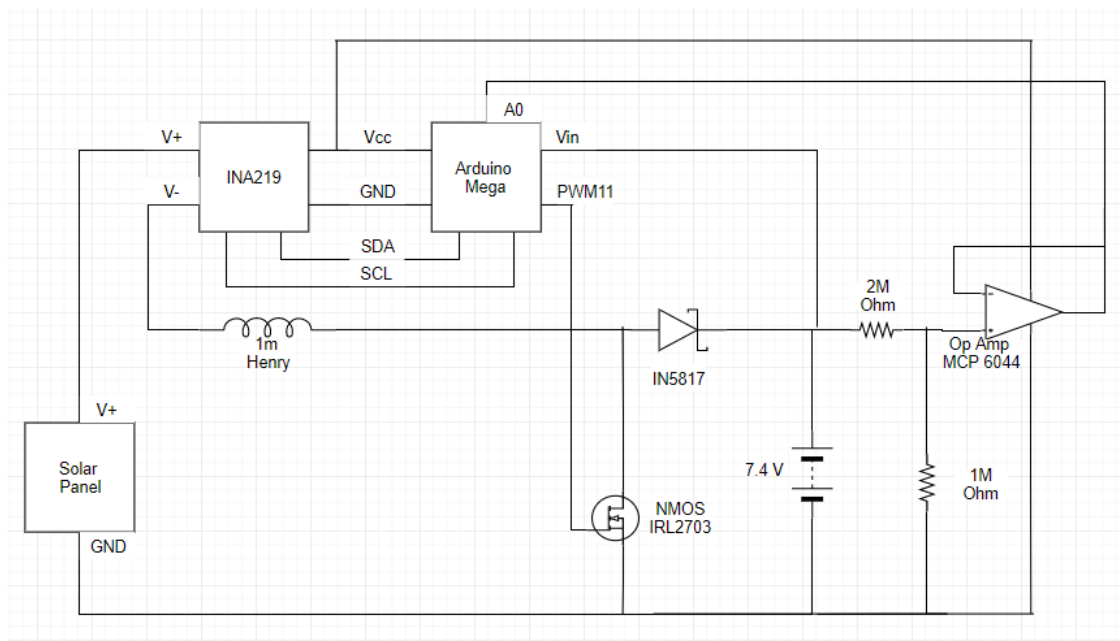


Figure 34 - Full Solar Charging System Schematic

The last main part of the system that needed to be designed was the maximum power point tracking algorithm, for this the perturb and observe (P&O) method was selected. The P&O method is very popular and is based on adjusting the duty cycle in order to vary the voltage and the observing if this change in voltage resulted in an increase or decrease in power (Femia, Petrone, Spagnuolo, & Vitelli, p. 42-43 2013). Depending on the observation, the next step will increase or decrease the duty cycle to increase the power. The time in between each perturbation as well as the change in the voltage with each step are important considerations (Femia, Petrone, Spagnuolo, & Vitelli, p. 43 2013). The P&O algorithm implemented changed the duty cycle by X each time, stepping the voltage by Y and waited Z seconds in between successive perturbations. The P&O algorithm implemented defined 5 conditions through if statements, summarized in the table below.

Table 26 - P&O Algorithm Summary

State	Power	Voltage	Action taken
Battery Overcharge	Non- zero	8.4 Volts (Battery)	Voltage to 0V
A	Increased	Decreased	Decrease voltage
B	Increased	Increased	Increase voltage
C	Decreased	Decreased	Increase voltage

D	Decreased	Increased	Decrease voltage
---	-----------	-----------	------------------

IMPLEMENTATION

Practical Model of the Solar Panel

Prior to actually implementing the 2W Voltaic Solar panel, the goal was to better understand the behavior of it with varying temperature and irradiance conditions. This was done by first extracting the parameters from the practical model. The practical model of a solar panel is represented by a current source, diode, shunt resistor and a series resistor shown in Figure 59 (Mahmoud, Xiao, & Zeineldin, 2013). The model used to find the values for the current source, shunt resistor, and series resistor was created by Mahmoud, Xiao, and Zeineldin and it strictly uses the data sheet values from the solar panel. Parameterization was done using the Newton Raphson approach to find Rs and Rsh and then the Is (short circuit current) and Ipho (photon current) could be determined.. The two equations used for the Newtown Raphson equation that resulted in finding Rs and Rsh are shown below and the script they are used in is in Appendix I: MATLAB Practical Model Parameter Extraction Code.

$$I_{sc} - I_m - \frac{V_m + I_m R_s}{R_{sh}} - \left(I_{sc} - \frac{V_{oc}}{R_{sh}} \right) \times \left[\exp \left(\frac{q(V_m + I_m R_s)}{N_s K T_o A} \right) - 1 \right] / \left[\exp \left(\frac{q V_{oc}}{N_s K T_o A} \right) - 1 \right] = 0$$

$$\frac{q \cdot e \cdot \frac{q V_m + I_m R_s}{N_s K T_o A}}{N_s \cdot K \cdot T_o \cdot A \cdot [e^{\frac{q V_{oc}}{N_s K T_o A}} - 1]} \times \left[\frac{I_m R_s V_{oc}}{V_m R_{sh}} - \frac{I_m R_s I_{sc}}{V_m} - \frac{V_{oc}}{R_{sh}} + I_{sc} \right] - \frac{I_m}{V_m} - \frac{I_m R_s}{V_m R_{sh}} + \frac{1}{R_{sh}} = 0$$

Here q is the electron charge, K is the Boltzmann constant, T is the Temperature of the module, Ns is the number of series cells, Iph is the photon current, Is is the saturation current, A is the ideality factor, Rs is the series resistance, Rsh is the shunt resistor, Im is the peak power current, Vm is the peak power voltage, and Voc is the open circuit voltage (Mahmoud, Xiao, & Zeineldin, 2013).

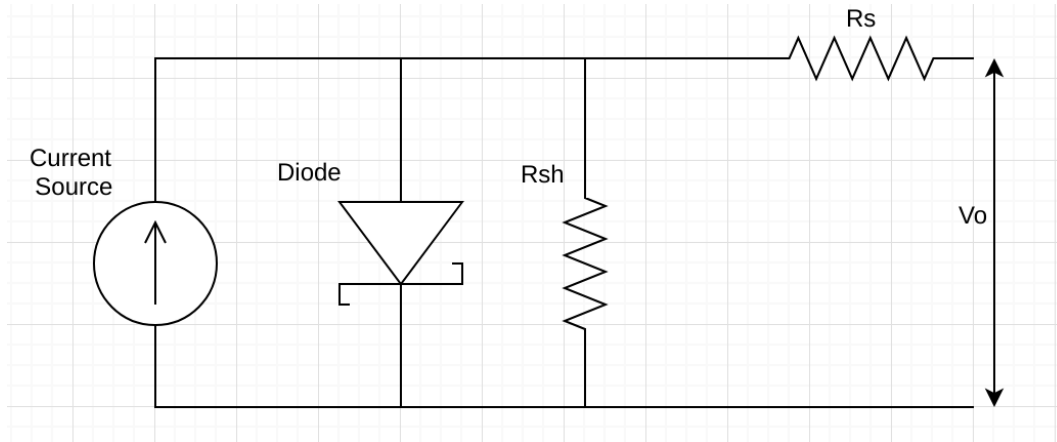


Figure 35 - Solar Panel Practical Model

Once the practical model for the solar panel was understood, the effects of the irradiance and temperature on the solar panel could be graphed. Increasing irradiance increases the power output of a solar panel and decreasing temperature increases the power output of a solar panel. Mahmoud, Xiao, and Zeineldin also derived an equation that can be used to model the effects of varying the temperature and irradiance on the PV and IV curves using the parameters extracted from the parameterization in the previous step, the formula is shown below.

$$I_S = \frac{e^{\frac{B\Delta T}{q}} G * (I_{sc} + \alpha \Delta T)}{\left(\frac{G I_{sc}}{I_{rs}} + 1\right)^{T_0/T} - e^{\frac{B\Delta T}{q}}}$$

In this equation ΔT is the temperature deviation from 298K, T_0 is the temperature at standard temperature, which is 298K. G is the irradiance, α is the temperature coefficient and B is the absolute value of the voltage temperature coefficient (Mahmoud, Xiao, & Zeineldin, 2013). This formula was applied in the MATLAB script shown in Appendix J: MATLAB Practical Model Characteristic Curve Plotting Code in order to get the resulting graphs shown below.

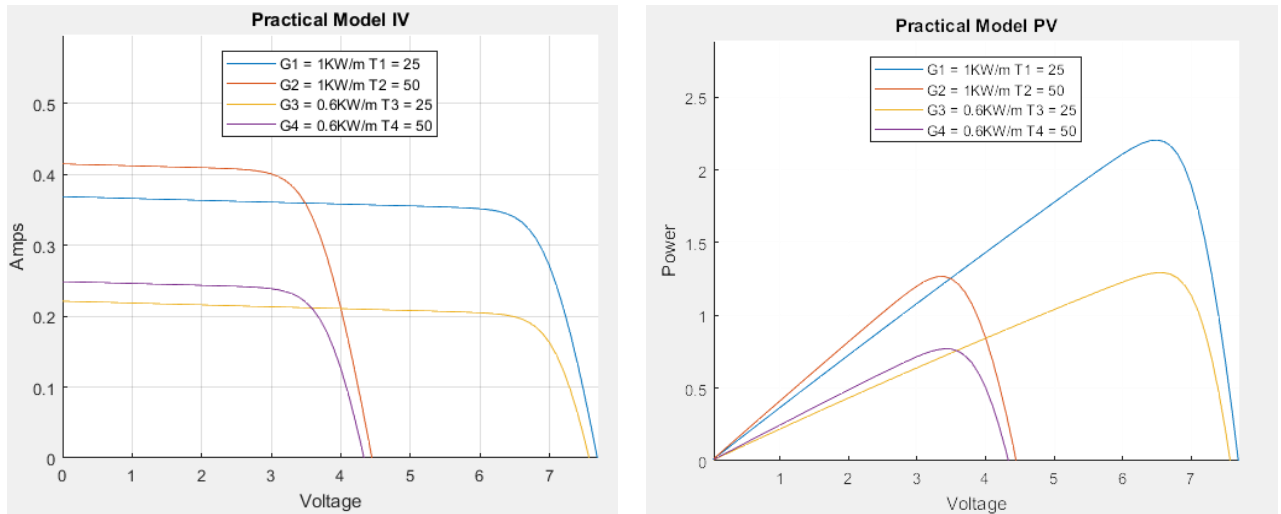
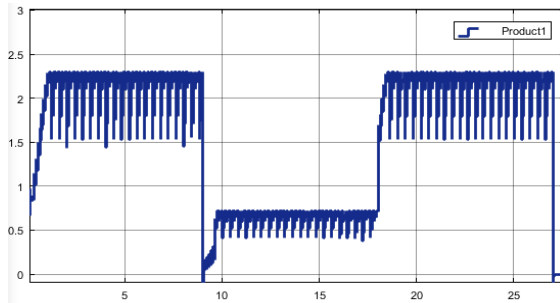


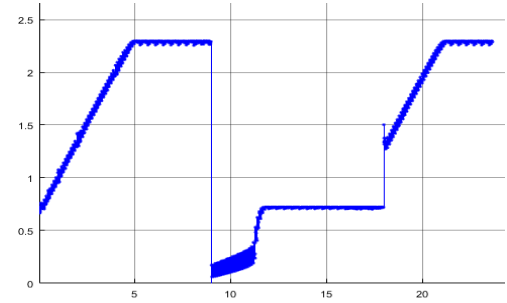
Figure 36 - Characteristic IV and PV Curves for Solar Panel

Simulation of the Solar Charging System

After understanding the model of the solar panel itself and the DC/DC Boost Converter, both were combined in a MATLAB Simulink Model. The model is shown in Appendix K (On Kayleah's Report): MATLAB Simulink Practical Model Solar Panel with DC/DC Converter. The code for the maximum power point tracking algorithm used in the model is in Appendix L: Maximum Power Point Tracking Code written in MATLAB. The Simulink model was used in order to verify the operation of the entire system. It was also used to adjust the parameters within the model and observe their effects on the output. One test that was done in Simulink was looking at the tradeoffs of increasing or decreasing the duty cycle step size. Two different duty cycle step sizes are shown in the figure below along with their Voltage vs Time curves, the change in the voltage is the result of the P&O algorithm searching for the new maximum power voltage operating point as a result of temperature increase and irradiance decrease (when the voltage went down) and temperature decrease and irradiance increase (when the voltage went back up).



Duty Cycle Step 0.05



Duty Cycle Step 0.01

Figure 37 –Duty Cycle Simulations

The notable observation from these graphs is that there is a tradeoff between the speed it takes to reach the maximum power and the oscillations around the maximum power once the voltage reaches the maximum power. When the duty cycle step size is large, maximum power is more rapidly found but there are larger oscillations around the maximum power point, causing loss of power. Methods do exist to vary the size of the duty cycle step based on proximity to the maximum power point, however these were not implemented.

Experimental Results from the Solar Charging System

The entire constructed system is shown in the figure below, the urban pollution mapping, the DC/DC converter, the battery, and the solar panel are highlighted.

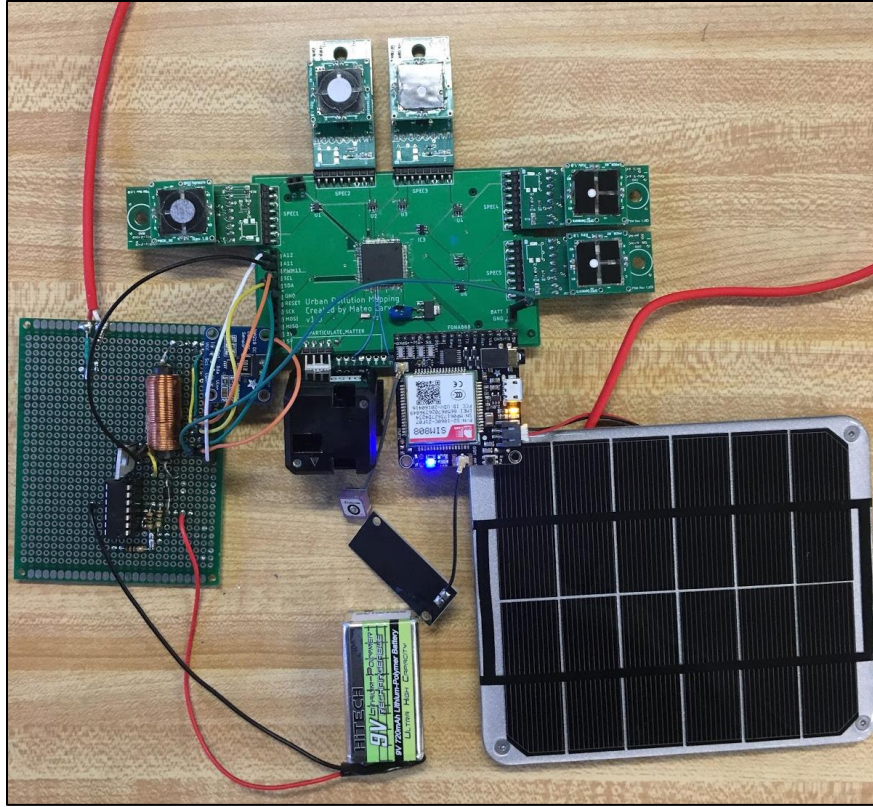


Figure 38 - Complete Prototype

Once the entire solar charging system was constructed, the characteristic IV and PV Curves were tested with a Halogen Lamp and the system voltage was monitored during changing irradiance conditions to see how the maximum power point tracking behaved. First the characteristic IV and PV curves were created by writing a MATLAB code that stepped through all of the possible duty cycles and the current, voltage and power of the solar panel were monitored. The characteristic curves are shown in the figure below.

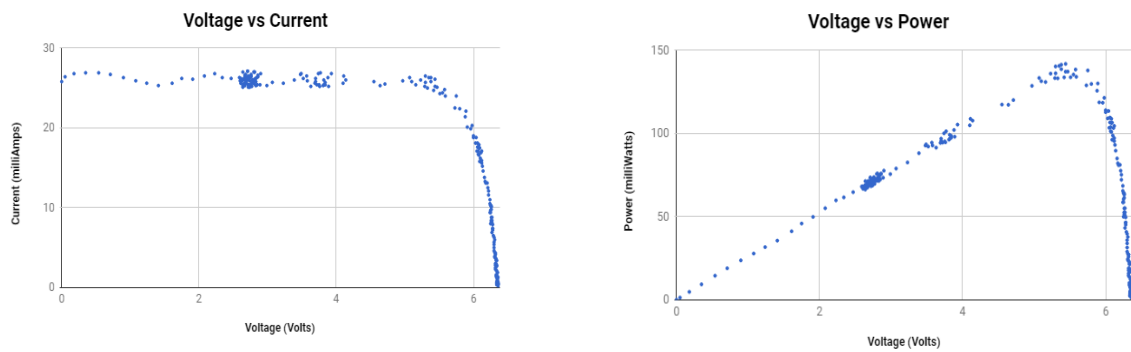


Figure 39 - The IV and PV Characteristic Curves for the Solar Panel

Due to the solar panel characteristics being tested under a Halogen light, the full power was not seen in the testing. However, the main goal of the duty cycle sweeping test was to ensure that the correct shape for the IV and PV curves were realized and they successfully were.

Next, the solar panels efforts to reach maximum power were observed. The figure below shows successive steps where with each step 1-6 the power output increased, however from 6- 7 the power decreased with an increase in the voltage so for the next step, 7-8, the voltage was decreased in order for it to recover its power, then in the last step 8-9 the voltage was decreased again to lead to a higher power output.

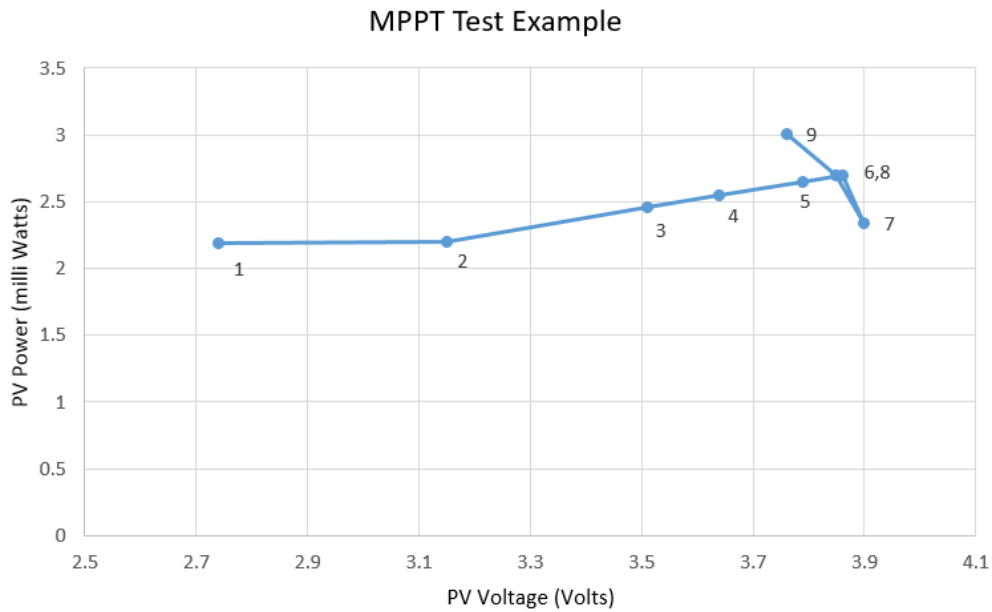


Figure 40 - Maximum Power Point Tracking Test Case

The last test that was conducted was to use the Halogen light and measure the voltage of the solar panel. Initially the halogen light was on at full intensity, then the Halogen light was shaded, and then the shading was removed to return the light to full intensity. The characteristic curve for this is shown in the figure below and a zoomed in portion of the rising voltage is shown on the right.

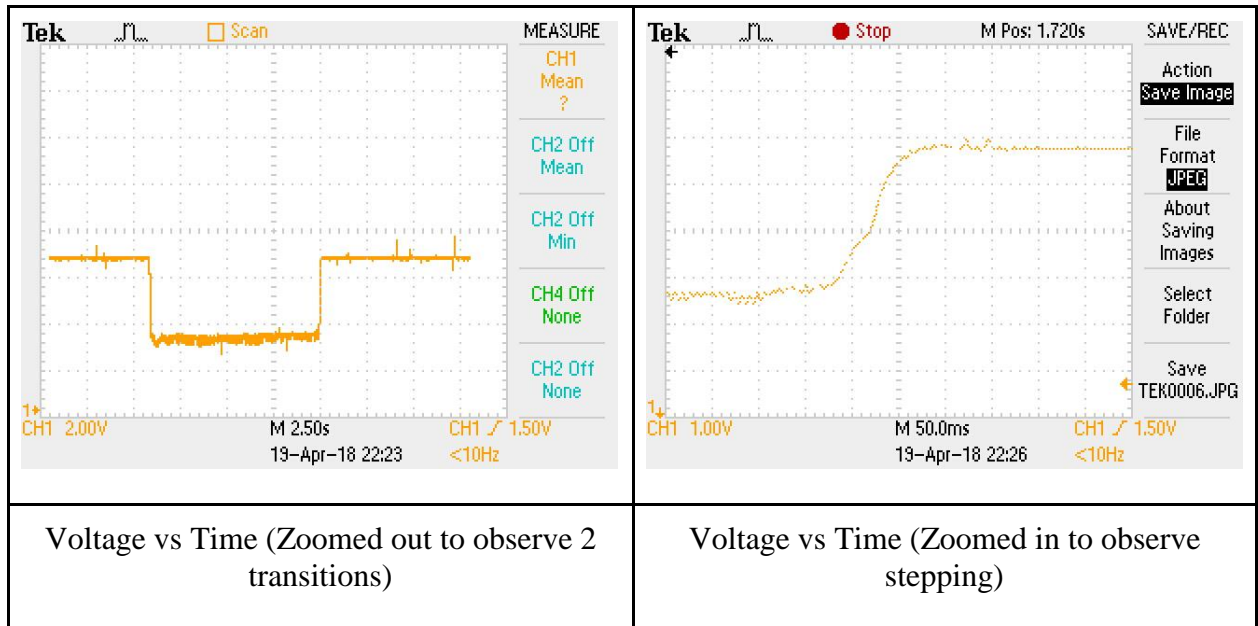


Figure 41 - Voltage Varying as a Result of Irradiance Level Changing

In this test the solar panel and maximum power point tracking algorithm worked as expected by adjusting the voltage when the irradiance changed. For the same irradiance values, the solar panel also kept the same voltage for the maximum power point.

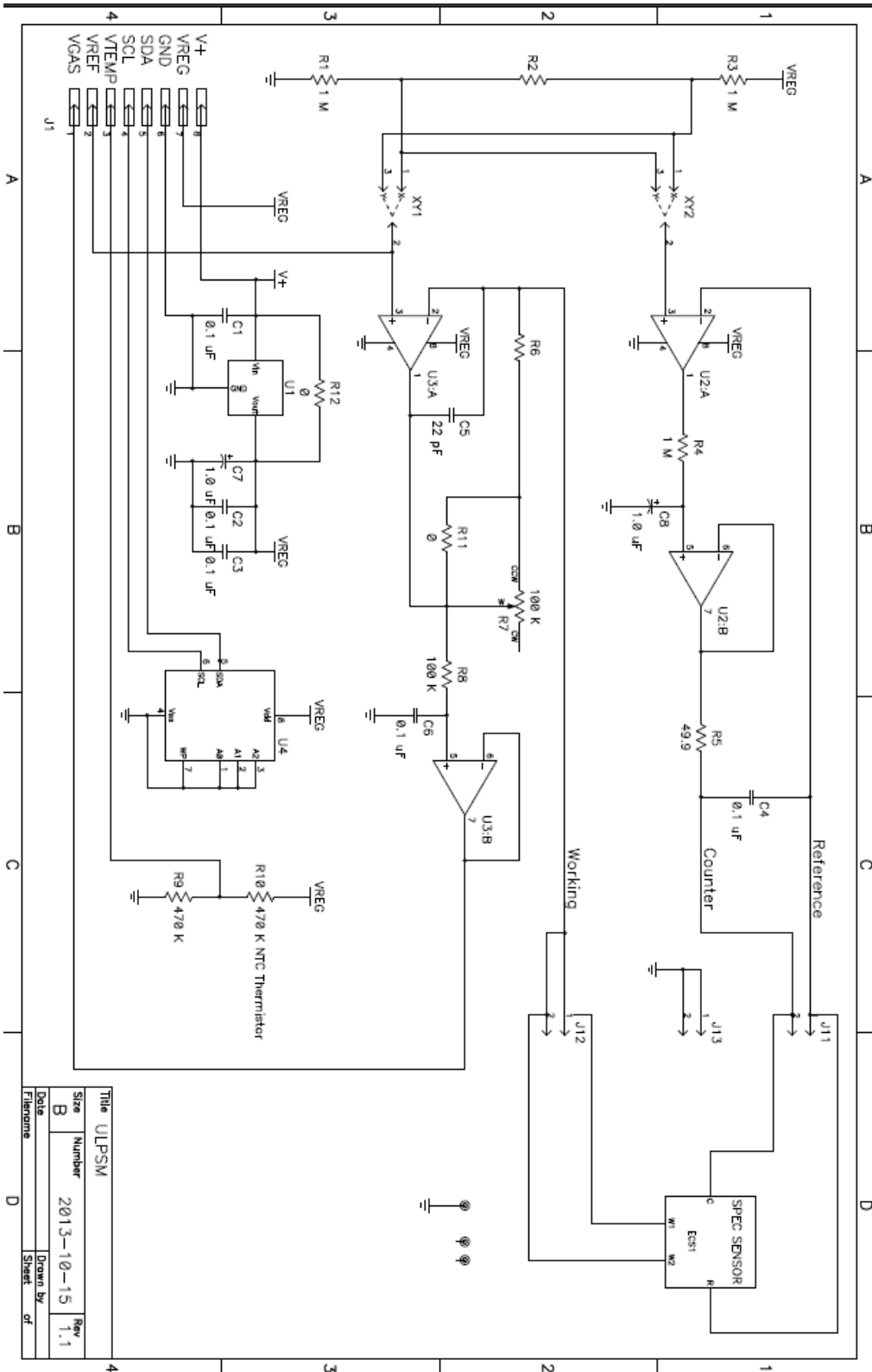
Recommendations for Future Work

Overall, the solar charging system was designed and implemented in order to provide the power system to the Urban Pollution Mapping device. Improvements to the system could certainly be made. The main areas that could be improved based on this project is the selection of the solar panel and the battery. Theoretically the selections were valid however practically the battery actually discharged rapidly. A solar panel that is rated for faster charging and a higher capacity battery would improve the project's success. Another improvement could be made would be by adjusting the maximum power point tracking algorithm. More duty cycle step sizes and wait times could be tested in order to select the best options for the system. The last improvement recommended is combining the urban pollution mapping subsystem and the solar charging subsystem into one printed circuit board to make the system a single packaged version.

Appendix B: Bill of Materials (BOM)

	Manufacturer Part Number	Manufacturer	Digi-Key Part Number	Quantity	Unit Price	Description
Microcontroller	ATMEGA2560-16AU	Microchip Technology	ATMEGA2560-16AU-ND	1	12.21	IC MCU 8BIT 256KB FLASH 100TQFP
3V Voltage Regulator	ADP3300ARTZ-3-RL7	Analog Devices Inc.	ADP3300ARTZ-3-RL7CT-ND	1	1.87	IC REG LINEAR 3V 50MA SOT23-6
Op-Amp	MCP6041T-E/OT	Microchip Technology	MCP6041T-E/OTCT-ND	6	0.58	IC OPAMP GP 14KHZ RRO SOT23-5
Header, Connector	PPPC021LFBN-RC	Sullins Connector Solutions	S7035-ND	2	0.33	CONN HEADER FEMALE 2POS .1" GOLD
Header, Connector	PPPC051LFBN-RC	Sullins Connector Solutions	S7038-ND	1	0.49	CONN HEADER FEMALE 5POS .1" GOLD
Header, Connector	PPPC071LFBN-RC	Sullins Connector Solutions	S7040-ND	1	0.61	CONN HEADER FEMALE 7POS .1" GOLD
5V Voltage Regulator	LM2940IMP-5.0/NOPB	Texas Instruments	LM2940IMP-5.0/NOPBCT-ND	1	2.17	IC REG LINEAR 5V 1A SOT223-4
Oscillator	ABLS-16.000MHZ-B4-T	Abracon LLC	535-10226-1-ND	1	0.25	CRYSTAL 16.000MHZ 18PF SMD
O3 Sensor	968-046	SPEC Sensors, LLC	1684-1049-ND	1	50	SENSOR OZONE ANALOG VOLTAGE MOD
CO Sensor	968-001	SPEC Sensors, LLC	1684-1002-ND	1	50	SENSOR GAS CO ANALOG VLTG MOD
H2S Sensor	968-003	SPEC Sensors, LLC	1684-1011-ND	1	50	SENSOR HYD SULF ANALOG VLTG MOD
SO2 Sensor	968-006	SPEC Sensors, LLC	1684-1023-ND	1	50	SENSOR SULF DIOX ANALOG VLTG MOD
NO2 Sensor	968-047	SPEC Sensors, LLC	1684-1050-ND	1	50	SENSOR NITR DIOX ANALOG VLTG MOD
Particulate Matter Sensor	PPD71	Shinyei Technologies	NA	1	50	PARTICULATE MATTER SENSOR

Appendix C: ULPSM Schematic [9]



Appendix D: Code Listing

Main.cpp

```
/*
 * Project: Mapping Urban Pollution
 * Author: Mateo Carvajal
 * Worcester Polytechnic Institute
 *
 * Last Update: April 19th 2018
 *
 * Main file of the system. This file calls the different functions,
retrieves the data and then commandas the data to be sent to the
database.
 *
*/

#include <UbidotsFONA.h>
#include <LowPower.h>
#include "UbidotsFONA.h"
#include "mqpdef.h"

int count = 0;
int i = 0;
float lat;

SpecSensorsResults specResults[LOOPS];
GPSCoordinates coord[LOOPS];
pmSensorResults pmResults[LOOPS];
float batteryVoltage[LOOPS];

void setup() {
  // put your setup code here, to run once:
  Serial.begin(9600); //used for communicating with Serial Monitor
  Serial3.begin(9600); //used for communicating with PM sensor

  Serial.println("Running Setup...");
  setup_spec();
  setup_ubidots();
  setup_power();
  Serial.println("All setup is complete!");
}

void loop() {
  if (count < LOOPS) {
    coord[count] = getGPS();
    lat = coord[count].latitude;
    specResults[count] = get_spec();
    pmResults[count] = get_pm();
    batteryVoltage[count] = loop_power();
    count++;
  }
  else {
    while (i < LOOPS) {
```

```

        send2Ubidots(specResults[i], coord[i], pmResults[i],
batteryVoltage[i]);
        i++;
    }
    count = 0;
    i = 0;
}

delay(1000);
}

```

Mqpdef.h

```

/*
 * Project: Mapping Urban Pollution
 * Author: Mateo Carvajal
 * Worcester Polytechnic Institute
 *
 * Last Update: April 19th 2018
 *
 * This header file defines a number of data structure and assigns
values to constants.
 */
#ifndef mqpdef_h
#define mqpdef_h

#include "Arduino.h"
// #include "Adafruit_FONA.h"
// #include <SoftwareSerial.h>

/*
 * General
 * ADCRESOLUTION = 1.1/2^10 = 1.1/1024 = 0.00107421875
 * ADCRESOLUTION = 3/2^10 = 3/1024 = 0.00322265625
 * DEBUG
 */
#define DEBUG false //When true Debug Information is printed to the
serial port.
#define ADC_RESOLUTION 0.00292968 // ADC_RESOLUTION = 3V / 1024
#define LOOPS 5

/* SPEC Sensor
 * CO
 * NO2
 * SO2
 * H2S
 * O3
 *
 * VREF
 * VGAS
 */
//TABLE BELOW | Arduino Mega
| AtMega2560 Direct

```

```

#define SPEC_VREF_PIN_CO 55 //ADC1 A1 55
63
#define SPEC_VGAS_PIN_CO 54 //ADC0 PIN(A0) = 54 else 97 A0 54
[Switch] 64
#define SPEC_VREF_PIN_NO2 57 // A3 57
61
#define SPEC_VGAS_PIN_NO2 56 // A2 56
62
#define SPEC_VREF_PIN_SO2 59 // A5 59
59
#define SPEC_VGAS_PIN_SO2 58 // A4 58
60
#define SPEC_VREF_PIN_H2S 61 // A7 61
57
#define SPEC_VGAS_PIN_H2S 60 // A6 60
58
#define SPEC_VGAS_PIN_O3 63 // A9 63
55
#define SPEC_VREF_PIN_O3 62 // A8 62
56
#define SPEC_VTEMP_PIN_O3 64 //Vtemp A10 64
54

//#define SPEC_SENSITIVITY_CODE_CO 4.44
//#define SPEC_SENSITIVITY_CODE_NO2 23.81
//#define SPEC_SENSITIVITY_CODE_SO2 36.58
//#define SPEC_SENSITIVITY_CODE_H2S 267.86
//#define SPEC_SENSITIVITY_CODE_O3 -72.04
//
//#define SPEC_TIA_GAIN_CO 100
//#define SPEC_TIA_GAIN_NO2 49.9
//#define SPEC_TIA_GAIN_SO2 499
//#define SPEC_TIA_GAIN_H2S 100
//#define SPEC_TIA_GAIN_O3 499

/*
 * The following values are the result of
 * M= SensitivityCode * TIAGain * 10^-9 *10^3
 * SPEC_CONSTANT_1_M = 1/M
 */
#define SPEC_CONSTANT_1_M_CO 2252.252
#define SPEC_CONSTANT_1_M_NO2 -841.667
#define SPEC_CONSTANT_1_M_SO2 54.784
#define SPEC_CONSTANT_1_M_H2S -37.333
#define SPEC_CONSTANT_1_M_O3 -27.818

//TEMPERATURE
#define BCOEFFICIENT 4500 //Specific to the Thermistor
#define TEMPERATURENOMINAL 25 //Room Temperature
#define THERMISTORNOMINAL 470000 //470 kOhm

/* GPS and 3G*/
#define FONA_RX 2
#define FONA_TX 10
#define FONA_RST 4

```

```

//SoftwareSerial fonaSS = SoftwareSerial(FONA_TX, FONA_RX);
//SoftwareSerial *fonaSerial = &fonaSS;

/* PM Sensor */

typedef struct pmSensorResults{
    uint8_t stx;
    uint8_t d1;
    uint8_t d2;
    uint8_t d3;
    uint16_t d4;
    uint16_t d5;
    uint16_t d6;
    uint16_t d7;
    uint16_t d8;
    uint16_t d9;
    uint16_t d10;
    uint16_t d11;
    uint16_t d12;
    uint32_t d13;
    uint8_t etx;
    uint8_t d14;
    uint8_t eot;
    float pm05_occupancy;
    float pm07_occupancy;
    float pm10_occupancy;
    float pm25_occupancy;
} ;//Measurements

//Spec functions
typedef struct SpecSensorsResults{
    float CO;
    float NO2;
    float SO2;
    float H2S;
    float O3;
    float TEMP;
};

void setup_spec();
SpecSensorsResults get_spec();
void specDebug(SpecSensorsResults specResults);

//GPS & 3G Functions
#define FONA_RX 2
#define FONA_TX 10
#define FONA_RST 4

//typedef struct GPSCoordinates{
//    float latitude;
//    float longitude;
//    float speed_kph;
//    float heading;
//    float altitude;
//};

```

```

//void setup_gps();
//GPSCoordinates get_gps();
pmSensorResults get_pm();

//Ubidots
void setup_ubidots();
GPSCoordinates getGPS();
void send2Ubidots(SpecSensorsResults specResults, GPSCoordinates coord,
pmSensorResults pmResults, float batteryVoltage );

//Power
void setup_power();
float loop_power();
void test_power (void) ;

#endif

```

SpecSensorCode.cpp

```

/*
 * Project: Mapping Urban Pollution
 * Author: Mateo Carvajal
 * Worcester Polytechnic Institute
 *
 * The following code was written to read and calculate the
concentration of five air pollutants:
 * 1. Carbon Monoxide
 * 2. Nitrogen Dioxide
 * 3. Sulphur Dioxide
 * 4. Hydrogen Sulphide
 * 5. Ozone
 *
 * The constants used in this file are declared in the 'mqpdef.h'
file.
 *
 * The function returns a pointer to a struct that holds the
concentration result for each air pollutant.
*/
#include "mqpdef.h"

float vref_co = 0;
float vgas_co = 0;
float vref_no2 = 0;
float vgas_no2 = 0;
float vref_so2 = 0;
float vgas_so2 = 0;
float vref_h2s = 0;
float vgas_h2s = 0;
float vref_o3 = 0;
float vgas_o3 = 0;
float temp_o3 = 0;
float tempVin = 0;

float concentration_co = 0;

```



```

float concentration_no2 = 0;
float concentration_so2 = 0;
float concentration_h2s = 0;
float concentration_o3 = 0;

float concentration_co_past = 0;
float concentration_no2_past = 0;
float concentration_so2_past = 0;
float concentration_h2s_past = 0;
float concentration_o3_past = 0;

void setup_spec(){
  Serial.println("Spec Setup...");
  analogReference(EXTERNAL); //Connected to the 3V Rail

  pinMode(SPEC_VREF_PIN_CO, INPUT);
  pinMode(SPEC_VGAS_PIN_CO, INPUT);
  pinMode(SPEC_VREF_PIN_NO2, INPUT);
  pinMode(SPEC_VGAS_PIN_NO2, INPUT);
  pinMode(SPEC_VREF_PIN_SO2, INPUT);
  pinMode(SPEC_VGAS_PIN_SO2, INPUT);
  pinMode(SPEC_VREF_PIN_H2S, INPUT);
  pinMode(SPEC_VGAS_PIN_H2S, INPUT);
  pinMode(SPEC_VTEMP_PIN_O3, INPUT);
  pinMode(SPEC_VREF_PIN_O3, INPUT);
  pinMode(SPEC_VGAS_PIN_O3, INPUT);
  Serial.println("SPEC SENSORS SETUP COMPLETE");
}

SpecSensorsResults get_spec(){

  SpecSensorsResults specResults;

  //Carbon Monoxide
  vref_co = analogRead(SPEC_VREF_PIN_CO) *ADC_RESOLUTION; // read
the input pin
  vgas_co = analogRead(SPEC_VGAS_PIN_CO) *ADC_RESOLUTION;
  concentration_co = (vgas_co - vref_co) * SPEC_CONSTANT_1_M_CO;

  //Nitrogen Dioxide
  vref_no2 = analogRead(SPEC_VREF_PIN_NO2) * ADC_RESOLUTION; //
read the input pin
  vgas_no2 = analogRead(SPEC_VGAS_PIN_NO2) * ADC_RESOLUTION;
  concentration_no2 = (vgas_no2 - vref_no2)*SPEC_CONSTANT_1_M_NO2;

  //Sulphur Dioxide
  vref_so2 = analogRead(SPEC_VREF_PIN_SO2) * ADC_RESOLUTION; //
read the input pin
  vgas_so2 = analogRead(SPEC_VGAS_PIN_SO2) * ADC_RESOLUTION;
  concentration_so2 = (vgas_so2 - vref_so2)*SPEC_CONSTANT_1_M_SO2;

  //Hydrogen Sulphide
  vref_h2s = analogRead(SPEC_VREF_PIN_H2S) * ADC_RESOLUTION; //
read the input pin
  vgas_h2s = analogRead(SPEC_VGAS_PIN_H2S) * ADC_RESOLUTION;
  concentration_h2s = (vgas_h2s - vref_h2s)*SPEC_CONSTANT_1_M_H2S;

```

```

//Ozone
vref_o3 = analogRead(SPEC_VREF_PIN_O3) * ADC_RESOLUTION; // read
the input pin
vgas_o3 = analogRead(SPEC_VGAS_PIN_O3) * ADC_RESOLUTION;
concentration_o3 = (vgas_o3 - vref_o3)*SPEC_CONSTANT_1_M_O3;

//Temperature
tempVin = analogRead(SPEC_VTEMP_PIN_O3) * ADC_RESOLUTION;
temp_o3 = (3 / tempVin) -1 ;
temp_o3 = log(temp_o3);
temp_o3 /= BCOEFFICIENT;
temp_o3 += 1.0 / (TEMPERATURENOMINAL + 273.15);
temp_o3 = 1.0 / temp_o3;
temp_o3 -= 273.15;

if(concentration_co >= 0){
    specResults.CO = concentration_co;
    concentration_co_past = concentration_co;
}
else{
    specResults.CO = concentration_co_past;
}
if(concentration_no2 >= 0.0){
    specResults.NO2 = concentration_no2;
    concentration_no2_past = concentration_no2;
}
else{
    specResults.NO2 = concentration_no2_past;
}
if(concentration_so2 >= 0.0){
    specResults.SO2 = concentration_so2;
    concentration_so2_past = concentration_so2;
}
else{
    specResults.SO2 = concentration_so2_past;
}
if(concentration_h2s >= 0.0){
    specResults.H2S = concentration_h2s;
    concentration_h2s_past = concentration_h2s;
}
else{
    specResults.H2S = concentration_h2s_past;
}
if(concentration_o3 >= 0.0){
    specResults.O3 = concentration_o3;
    concentration_o3_past = concentration_o3;
}
else{
    specResults.O3 = concentration_o3_past;
}

specResults.TEMP = temp_o3;

if(DEBUG){

```

```

        specDebug(specResults);
    }

    return specResults;
}

void specDebug(SpecSensorsResults specResults){
//  delay(1000);
    Serial.println("_____");

    Serial.print("Carbon Monoxide Concentration:  ");           //
    debug value
    Serial.print(specResults.CO,15);
    Serial.print(" ppm\n");

    Serial.print("Nitrogen Dioxide Concentration:  ");           //
    debug value
    Serial.print(specResults.NO2,15);
    Serial.print(" ppm\n");

    Serial.print("Sulphur Dioxide Concentration:  ");           //
    debug value
    Serial.print(specResults.SO2,15);
    Serial.print(" ppm\n");

    Serial.print("Hydrogen Sulphide Concentration:  ");           //
    debug value
    Serial.print(specResults.H2S,15);
    Serial.print(" ppm\n");

    Serial.print("Ozone Concentration:  ");                       //
    debug value
    Serial.print(specResults.O3,15);
    Serial.print(" ppm\n");
}

```

pmSensorCode.cpp

```

/*
 * Project: Mapping Urban Pollution
 * Author: Mateo Carvajal
 * Worcester Polytechnic Institute
 *
 * Last Update: Feb 6th 2018
 *
 * The following code works with a Shinyei PPD 71 Sensor. This sensor
is designed to measure particulate matter.
 * The following code only needs to have connected pins 1,3 and 4. Pin
2 is left open(not grounded).
 *
 * Pins
 * 1 -> GND
 * 2 -> Output Mode(Open- Automatic Transmission, Grounded- Command
Response Mode
 * 3 -> PWR 5V

```

```

* 4 -> TX (Output 3.3V)
* 5 -> RX (Input 3.3V)
*
* |-----| Bottom View
* | PM      |
* | SENSOR  |
* |-----|
* | 12345 pins
*/

#include "mqpdef.h"

//Buffer to store information from the sensor
char Buffer[29];
//pmSensorDataStructure pmLog[100];
//
//void setup() {
// //Setup Serial3 to communicate with Shinyei
// Serial.begin(9600);
// Serial3.begin(9600);
//}

/*
* pmSesorResults get_pm()
* returns the values obtained from the PMSensor as the occupancy
ratio.
*/

pmSensorResults get_pm(){
    pmSensorResults pmReading;

    //Data is received in bytes. It is put into the buffer array.
    if(Serial3.available()){
        Serial3.readBytesUntil('0x04', Buffer, 29);
    }

    //D3, D11 and D14 are represented in two bytes. Hence we take the
first byte,
    //shift it left by a byte and then OR it with the second byte.
    uint16_t d3 = (uint16_t)Buffer[3] << 8;
    d3 |= Buffer[4];
    // uint16_t d3 = d3_bigEndian ;//SwapBits(d3_bigEndian);

    // SwapBits(65281);

    uint16_t d4 = (uint16_t)Buffer[5] << 8;
    d4 |= Buffer[6];

    uint16_t d5 = (uint16_t)Buffer[7] << 8;
    d5 |= Buffer[8];

    uint16_t d6 = (uint16_t)Buffer[9] << 8;
    d6 |= Buffer[10];

    uint16_t d7 = (uint16_t)Buffer[11] << 8;
    d7 |= Buffer[12];

```

```

uint16_t d8 = (uint16_t)Buffer[13] << 8;
d8 |= Buffer[14];

uint16_t d9 = (uint16_t)Buffer[15] << 8;
d9 |= Buffer[16];

uint16_t d10 = (uint16_t)Buffer[17] << 8;
d10 |= Buffer[18];

uint16_t d11 = (uint16_t)Buffer[19] << 8;
d11 |= Buffer[20];

//D13 is 4 bytes long
uint32_t d13 = (uint32_t)Buffer[22]<<8; //First 16
d13 |= Buffer[23];
d13 << 8; //Second 24
d13 |= Buffer[24];
d13 << 8; //Third 32
d13 |= Buffer[25];

//Assignment of values to fields in the pmReading
pmReading.stx = (uint8_t)Buffer[0];
pmReading.d1 = (uint8_t)Buffer[1];
pmReading.d2 = (uint8_t)Buffer[2];
pmReading.d3 = d3;
pmReading.d4 = d4;
pmReading.d5 = d5;
pmReading.d6 = d6;
pmReading.d7 = d7;
pmReading.d8 = d8;
pmReading.d9 = d9;
pmReading.d10= d10;
pmReading.d11= d11;
pmReading.d12= (uint8_t)Buffer[21];
pmReading.d13= d13;
pmReading.etx= (uint8_t)Buffer[26];
pmReading.d14= (uint8_t)Buffer[27];
pmReading.eot= (uint8_t)Buffer[28];
pmReading.pm05_occupancy = d7/10000;
pmReading.pm07_occupancy = d8/10000;
pmReading.pm10_occupancy = d9/10000;
pmReading.pm25_occupancy = d10/10000;

if(DEBUG){
    printValues(pmReading);
}

return pmReading;
}

/*
 * printValues()
 * @param pmSensorDataStructure pmData

```

```

* @return void
*
* The following function is called if DEBUG is true. It will print out
all the values received to the buffer.
*/
void printValues(pmSensorResults pmData){
    Serial.println("_____");
    Serial.println("Debugging");
    Serial.print("D1  Number of Bytes Transmitted:");
    Serial.println(pmData.d1);
    Serial.print("D2  Command(Fixed Value):      ");
    Serial.println(pmData.d2);

    Serial.print("D3  Mass Concentration 10s:      ");
    Serial.println(pmData.d3);
    Serial.print("D4  Mass Concentration 30s:      ");
    Serial.println(pmData.d4);
    Serial.print("D5  Mass Concentration 60s:      ");
    Serial.println(pmData.d5);
    Serial.print("D6  Mass Concentration 180s:     ");
    Serial.println(pmData.d6);
    Serial.print("D7  0.5um Pulse Ratio Output:      ");
    Serial.println(pmData.d7);
    Serial.print("D8  0.7um Pulse Ratio Output:      ");
    Serial.println(pmData.d8);
    Serial.print("D9  1.0um Pulse Ratio Output:      ");
    Serial.println(pmData.d9);
    Serial.print("D10 2.5um Pulse Ratio Output:      ");
    Serial.println(pmData.d10);
    Serial.print("D11 Status:                          ");
    Serial.println(pmData.d11);
    Serial.print("D12 Software Version:                ");
    Serial.println(pmData.d12);
    Serial.print("D13 Production Number:              ");
    Serial.println(pmData.d13);
    Serial.print("ETX:                                ");
    Serial.println(pmData.etx);
    Serial.print("D14 Checksum:                          ");
    Serial.println(pmData.d14);
    Serial.print("EOT:                                ");
    Serial.println(pmData.eot);

    Serial.print("PM 0.5 Occupancy:                      ");
    Serial.println(pmData.pm05_occupancy);
    Serial.print("PM 2.5 Occupancy:                      ");
    Serial.println(pmData.pm25_occupancy);
}

```

Power.cpp

```

/*
* Project: Mapping Urban Pollution
* Author: Kayleah Griffen
* Worcester Polytechnic Institute
*

```

```

* Last Update: April 19th 2018
*
* The following codes takes care of monitoring the power of
* the solar panel and charging the battery. It charges the battery
using
* maximum power point tracking(MPPT)
*
*/
#include <Wire.h>
#include <Adafruit_INA219.h>
#include "mqpdef.h"

Adafruit_INA219 ina219_PV;
//Adafruit_INA219 ina219_Battery(0x41);

int pin = 11;
//float current_mA;

float Power;
float Old_Power;

int Duty_Cycle;
int Dstep;
int Duty_Cycle_Cutoff;

float Voltage;
float Old_Voltage;

float current_mA;
float Old_Current;

float Battery_Voltage;
//float Battery_Current = 0;

//int Max_Battery_Current = 370;
float Max_Battery_Voltage = 8.4;

float Other_power;

int sensorValue;
float voltage;

void setup_power(void) {

    Duty_Cycle = 40;
    Dstep = 1 ;
    Duty_Cycle_Cutoff = 0;
    Old_Voltage = 0;
    current_mA = 0;

    Battery_Voltage = 0;

```

```

Max_Battery_Voltage = 8.4;

int myEraser = 7; // this is 111 in binary and is
used as an eraser
TCCR1B &= ~myEraser; // this operation (AND plus NOT), set the
three bits in TCCR1B to 0
int myPrescaler = 1; // this could be a number in [1 , 6].
In this case, 3 corresponds in binary to 011.
TCCR1B |= myPrescaler; //this operation (OR), replaces the last
three bits in TCCR2B with our new value 011
Serial.begin(9600);

analogReference(EXTERNAL);
Serial.println("Hello!");

// Initialize the INA219.
// By default the initialization will use the largest range (32V,
2A). However
// you can call a setCalibration function to change this range (see
comments).
ina219_PV.begin();
//ina219_Battery.begin();

// To use a slightly lower 32V, 1A range (higher precision on amps):
//ina219.setCalibration_32V_1A();
// Or to use a lower 16V, 400mA range (higher precision on volts and
amps):
ina219_PV.setCalibration_16V_400mA();
//ina219_Battery.setCalibration_16V_400mA();
Serial.println("Setup complete");
}

float loop_power(){

analogWrite(pin, Duty_Cycle) ;

Old_Power = Old_Voltage * Old_Current;

Voltage = ina219_PV.getBusVoltage_V();
current_mA = ina219_PV.getCurrent_mA();
Power = Voltage * current_mA;
Other_power = ina219_PV.getPower_mW();
sensorValue = analogRead(A11);
// Convert the analog reading (which goes from 0 - 1023) to a voltage
(0 - 5V):
voltage = sensorValue * (3.0 / 1023.0) * 3;
// print out the value you read:

Serial.print("Duty Cycle: "); Serial.print(Duty_Cycle);
Serial.println("/256");
Serial.print("PV Voltage: "); Serial.print(Voltage);
Serial.println(" V");
Serial.print("PV Current: "); Serial.print(current_mA);
Serial.println(" mA");
Serial.print("PV Power: "); Serial.print(Power);
Serial.println(" mW");

```



```

    Serial.print("Old Voltage:      "); Serial.print(Old_Voltage);
    Serial.println(" V");
    Serial.print("Old Power:       "); Serial.print(Old_Power);
    Serial.println(" mW");

    Serial.print("Battery Voltage:  "); Serial.print(voltage);
    Serial.println(" V");

    if (Duty_Cycle < 0){
        Duty_Cycle = 10; //resetting up a little higher to prevent negative
    }

    if ((Power > Old_Power) and (Voltage > Old_Voltage)) {
        Duty_Cycle = Duty_Cycle - Dstep;
        Serial.println("A");
    }

    //Increasing power, Decreasing Voltage
    //keep decreasing volgate by increasing duty cycle
    else if ((Power >= Old_Power) and (Voltage <= Old_Voltage)) {
        Duty_Cycle = Duty_Cycle + Dstep;
        Serial.println("B");
    }

    //Decreasing power, Increasing Voltage
    //instead decrease volgate by increasing duty cycle
    else if ((Power < Old_Power) and (Voltage >= Old_Voltage)) {
        Duty_Cycle = Duty_Cycle + Dstep;
        Serial.println("C");
    }

    //Decreasing power, Decreasing Voltage
    //instead increase volgate by decreasing duty cycle
    else if ((Power < Old_Power) and (Voltage <= Old_Voltage)) {
        Duty_Cycle = Duty_Cycle - Dstep;
        Serial.println("D");
    }

    analogWrite(pin, Duty_Cycle) ;// use pins 12 or 11
    Serial.println("");

    //set the olds
    Old_Power = Power;
    Old_Voltage = Voltage;
    Old_Current = current_mA;

    return Voltage;
}

void test_power (void) {
    Duty_Cycle = 0;
    int max_duty_cycle = 256;
    while (max_duty_cycle > Duty_Cycle){
        analogWrite(pin, Duty_Cycle) ;

```

```

    Voltage = ina219_PV.getBusVoltage_V();
    current_mA = ina219_PV.getCurrent_mA();
    Power = Voltage * current_mA;
    Other_power = ina219_PV.getPower_mW();
    Serial.print("Duty Cycle:      "); Serial.print(Duty_Cycle);
Serial.println("/256");
    Serial.print("PV Voltage:      "); Serial.print(Voltage);
Serial.println(" V");
    Serial.print("PV Current:      "); Serial.print(current_mA);
Serial.println(" mA");
    Serial.print("PV Power:        "); Serial.print(Power);
Serial.println(" mW");
    Serial.print("Other PV Power:   "); Serial.print(Other_power);
Serial.println(" mW");
    Duty_Cycle = Duty_Cycle + 1;
}
}

```

Ubidots.cpp

```

/*
 * Project: Mapping Urban Pollution
 * Author: Mateo Carvajal
 * Worcester Polytechnic Institute
 *
 * Last Update: April 19th 2018
 *
 * The following code works with the FONA 808 GPS & 3G Module
 * It contains functions to:  Retrieve the GPS location
 *                            Send the data to the database
 *
 * The code is based from Ubidots code examples.
 */

#include "UbidotsFONA.h"
#include "mqpdef.h"
#include <stdio.h>

#define APN "wholesale" // The APN of your operator
#define USER "" // if your apn doesnt have username just leave it ""
#define PASS "" // if your apn doesnt have password just leave it ""
#define TOKEN "A1E-e410VDZ0TBihwsxssuJxPltjnjdBlL" // Replace it with
your Ubidots token
#define VARIABLE_LABEL_1 "CO2" // Replace it with your Ubidots variable
label
#define VARIABLE_LABEL_2 "NO2" // Replace it with your Ubidots variable
label
#define VARIABLE_LABEL_3 "SO2" // Replace it with your Ubidots variable
label
#define VARIABLE_LABEL_3 "H2S"
#define VARIABLE_LABEL_3 "O3"

```

```

Ubidots client(TOKEN);

void setup_ubidots() {
  Serial.println("Ubidots Setup...");
  delay(1000); //2000
  client.setDebug(DEBUG); // comment this line to set DEBUG off
  while(!client.setApn(APN, USER, PASS));
  client.setupGPS();
}

GPSCoordinates getGPS(){
  return client.getGPS();
}

void send2Ubidots(SpecSensorsResults specResults, GPSCoordinates coord,
pmSensorResults pmResults, float batteryVoltage ) {
  char latContext[14];
  char lngContext[14];
  char context[50];
  float lat = coord.latitude;
  float lng = coord.longitude;

  dtostrf(lat, 7, 3, latContext);
  dtostrf(lng, 7, 3, lngContext);

  sprintf(context, "lat=%s$lng=%s", latContext, lngContext);
  Serial.println(context);
  Serial.println("Sending Data");
  client.add("CO" , specResults.CO);
  client.add("NO2" , specResults.NO2);
  client.add("SO2" , specResults.SO2);
  client.add("H2S" , specResults.H2S);
  client.add("O3" , specResults.O3);
  client.add("Temp", specResults.TEMP);
  client.add("PM2.5", pmResults.pm25_occupancy);
  client.add("PM0.5", pmResults.pm05_occupancy);
  client.add("Coordinates", 1.00, context);
  client.add("Batt Voltage", batteryVoltage);

  Serial.println(context);
  Serial.println(coord.latitude);
  if(client.sendAll()){
    Serial.println("values sent properly");
  }
}

//void debug_gps(GPSCoordinates coord) {
//  Serial.println(coord.latitude, 6);
//  Serial.println(coord.longitude, 6);
//  Serial.println(coord.speed_kph);
//  Serial.println(coord.heading);
//  Serial.println(coord.altitude);
//}

```

Appendix E: MATLAB Practical Model Parameter Extraction Code

```
%Practical PV model
%Parameters Iph, Is, Rs, and Rsh are found through 4 equations and A is
%assumed to be 1.3

%CURRENT AND VOLTAGE FROM IN CLASS EXAMPLE PV MODULE

function F = solving(x)

%constants
q = 1.60217657e-19;
K = 1.3806488e-23;

Voc = 7.7;
Vm = 6.5;
Isc = 0.370;
Im = 0.340;
Ns = 12;

T = 25+273;
A = .7;

%define variables to be solved using the Newton Raphson equations
Rs = x(1);
Rsh = x(2);

F(1)=Isc-Im-(Vm+Im*Rs)/Rsh-(Isc-Voc/Rsh)*(exp(q*(Vm+Im*Rs)/(Ns*K*T*A))-
1)/(exp(q*Voc/(Ns*K*T*A))-1) ;
F(2)= exp(q*(Vm+Im*Rs)/(Ns*K*T*A))*(q*Im*Rs*Voc/(Ns*K*T*A*Vm*Rsh)-q*Im*Rs*Isc/(Ns*K*T*A*Vm)-
q*Voc/(Ns*K*T*A*Rsh)+q*Isc/(Ns*K*T*A))/(exp(q*Voc/(Ns*K*T*A))-1)-Im/Vm-Im*Rs/(Rsh*Vm)+1/Rsh;

%printing of all the values
Rs
Rsh
Ipho = Isc
Iso = (Ipho-(Voc/Rsh))/((exp((q*Voc)/(Ns*K*T*A))-1))
end
```

Appendix F: MATLAB Practical Model Characteristic Curve Plotting Code

```
%Practical model
%Plots of IV and PV curves at various conditions for given G and T
%Parameters taken from Assig1_Practical_Model
Rs = 0.5274;
Rsh =331.8286;
Ipho = 8.2300;
Iso = 8.3538e-15;

%constants
q = 1.60217657e-19;
K = 1.3806488e-23;
Voc = 33.5;
Vm = 26.3;
Isc = 8.23;
Im = 7.8;
Ns = 54;
T = 25+273;
A = .7;
alpha = 0.5/100*Isc;
B = -0.116;

%G1 = 1KW/m T1 = 25
G1= 1;
T1 = 25 + 273;
Iph1 = G1*(Ipho+alpha*(T1-T));
Is1 = Ipho/(exp(q*(Voc - (abs(B)*(T1-T)))/(Ns*K*T1*A))-1);

%G2 = 1KW/m T2 = 50
G2 = 1;
T2 = 50+ 273;
Iph2 = G2*(Ipho+alpha*(T2-T));
Is2 = Ipho/(exp(q*(Voc - (abs(B)*(T2-T)))/(Ns*K*T2*A))-1);

%G3 = 0.6KW/m T3 = 25
G3 = 0.6;
T3 = 25+ 273;
Iph3 = G3*(Ipho+alpha*(T3-T));
Is3 = Ipho/(exp(q*(Voc - (abs(B)*(T3-T)))/(Ns*K*T3*A))-1);

%G4 = 0.6KW/m T3 = 50
G4 = 0.6;
T4 = 50+ 273;
Iph4 = G4*(Ipho+alpha*(T4-T));
Is4 = Ipho/(exp(q*(Voc - (abs(B)*(T4-T)))/(Ns*K*T4*A))-1);

%plotting the results
X = 0: .1: Voc;
```

```

syms C;
c = 8;

for i = 1:length(X)
%use Newton - Raphson method to find current
F(C) = Iph1 - C- Is1*((exp((q*(X(i)+ C*Rs))/(Ns*K*T*A))-1)) - (X(i)+ C*Rs)/Rsh ;
Fd(C) = diff(F(C));
ans1 = double(F(c));
ans2 = double(Fd(c));
while abs(ans1) > 1e-6
c = double(c - ans1/ans2);
ans1 = double(F(c));
ans2 = double(Fd(c));
end
I1(i) = c;
P1(i) = c * X(i);
end

syms D;
d = 8;

for i = 1:length(X)
%use Newton - Raphson method to find current
F(D) = Iph2 - D- Is2*((exp((q*(X(i)+ D*Rs))/(Ns*K*T*A))-1)) - (X(i)+ D*Rs)/Rsh ;
Fd(D) = diff(F(D));
ans1 = double(F(d));
ans2 = double(Fd(d));
while abs(ans1) > 1e-6
d = double(d - ans1/ans2);
ans1 = double(F(d));
ans2 = double(Fd(d));
end
I2(i) = d;
P2(i) = d * X(i);
end

syms D;
d = 4;

for i = 1:length(X)
%use Newton - Raphson method to find current
F(D) = Iph3 - D- Is3*((exp((q*(X(i)+ D*Rs))/(Ns*K*T*A))-1)) - (X(i)+ D*Rs)/Rsh ;
Fd(D) = diff(F(D));
ans1 = double(F(d));
ans2 = double(Fd(d));
while abs(ans1) > 1e-6
d = double(d - ans1/ans2);
ans1 = double(F(d));
ans2 = double(Fd(d));
end
I3(i) = d;
P3(i) = d * X(i);
end

syms D;
d = 8;

```

```

for i = 1:length(X)
%use Newton - Raphson method to find current
F(D) = Iph4 - D- Is4*((exp((q*(X(i)+ D*Rs))/(Ns*K*T*A))-1)) - (X(i)+ D*Rs)/Rsh ;
Fd(D) = diff(F(D));
ans1 = double(F(d));
ans2 = double(Fd(d));
while abs(ans1) > 1e-6
d = double(d - ans1/ans2);
ans1 = double(F(d));
ans2 = double(Fd(d));
end
I4(i) = d;
P4(i) = d * X(i);
end

```

```

figure(1)
hold on
a1 = plot(X,I1); M1 = "G1 = 1KW/m T1 = 25";
a2 = plot(X,I2); M2 = "G2 = 1KW/m T2 = 50";
a3 = plot(X,I3); M3 = "G3 = 0.6KW/m T3 = 25";
a4 = plot(X,I4); M4 = "G4 = 0.6KW/m T4 = 50";

xlim([0 Voc])
ylim([0 10])

legend([a1,a2, a3, a4], [M1, M2, M3, M4], 'Location', 'South');

```

```

title('Practical Model IV')
grid on
xlabel('Voltage')
ylabel('Amps')
hold off

```

```

figure(2)
hold on
a1 = plot(X,P1); M1 = "G1 = 1KW/m T1 = 25";
a2 = plot(X,P2); M2 = "G2 = 1KW/m T2 = 50";
a3 = plot(X,P3); M3 = "G3 = 0.6KW/m T3 = 25";
a4 = plot(X,P4); M4 = "G4 = 0.6KW/m T4 = 50";

xlim([0 Voc])
ylim([0 250])

legend([a1,a2, a3, a4], [M1, M2, M3, M4], 'Location', 'South');

```

```

title('Practical Model PV')
grid on
xlabel('Power')

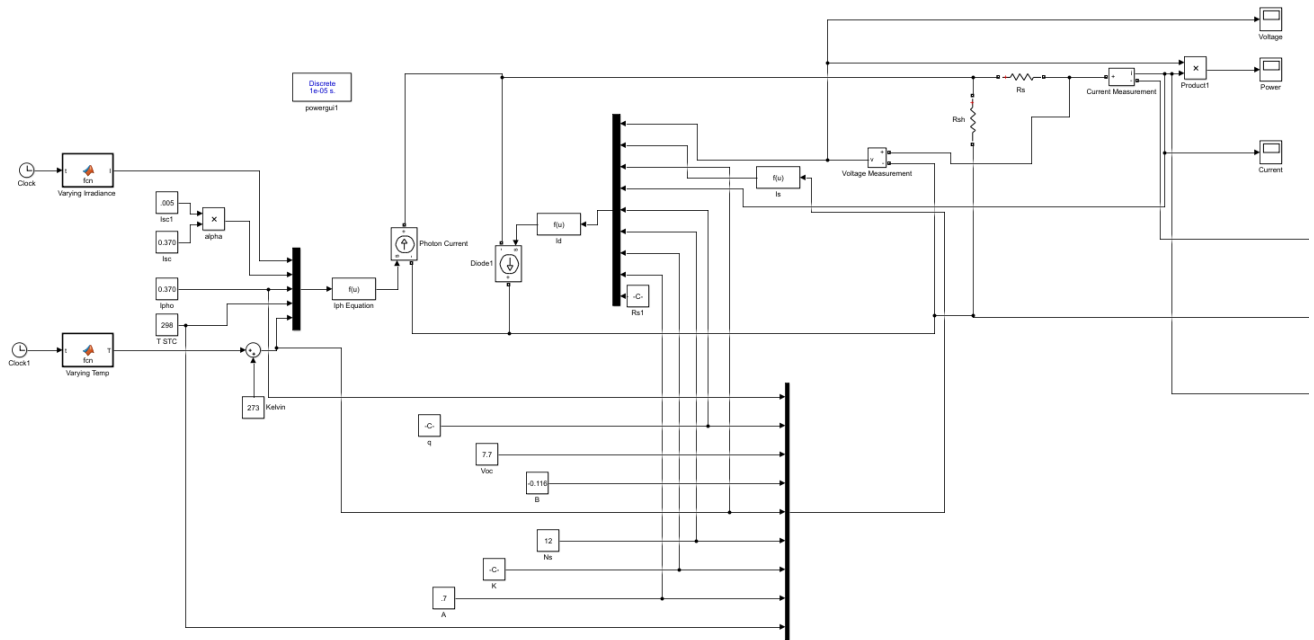
```

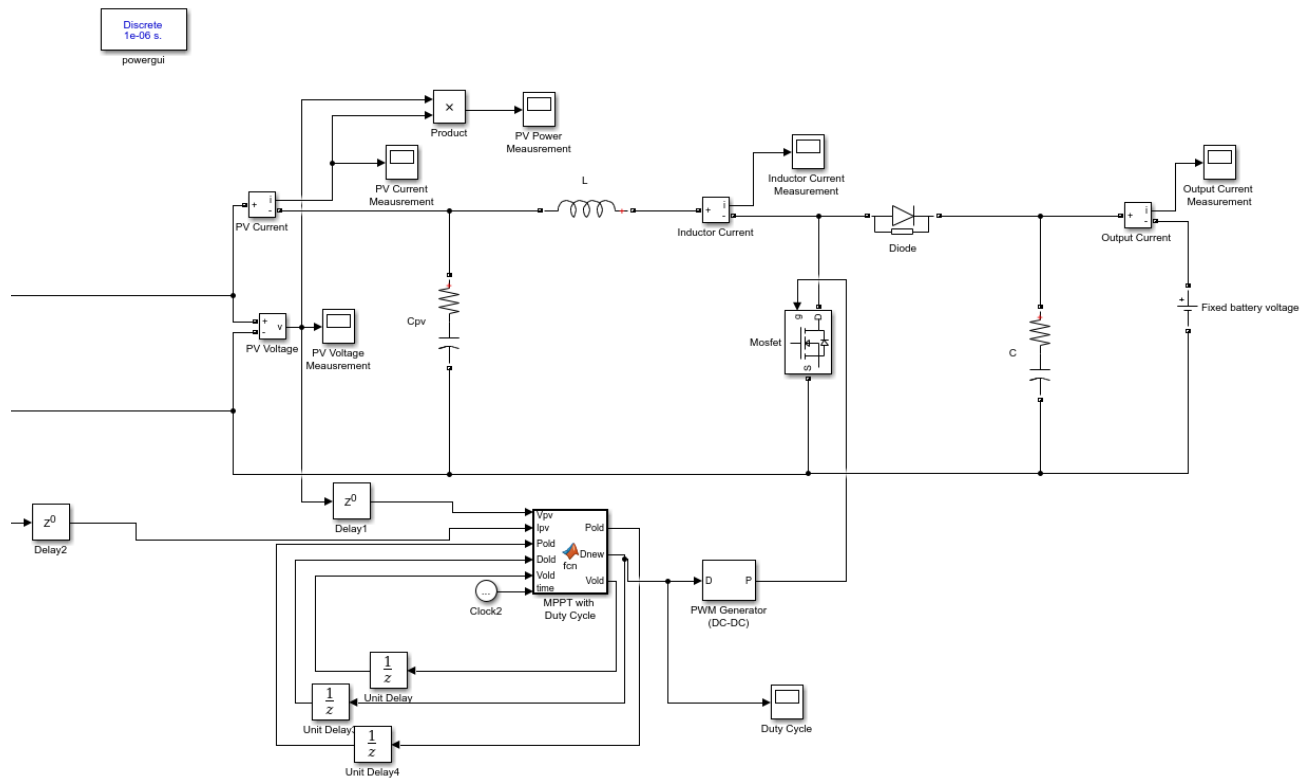
```

ylabel('Amps')
hold off

```

Appendix G: MATLAB Simulink Practical Model Solar Panel with DC to DC Converter





Appendix H: Maximum Power Point Tracking Code written in MATLAB

```
function [Pold, Dnew, Vold] = fcn(Vpv, Ipv, Pold, Dold, Vold, time)

%The duty cycle actually should only range from
%a maximum of 1 to a minimum of 0.665
%V = 0 at D = 1 and Voc 33.5 at D = 0.665
%governing equation Vpv = Vo*(1-D)

%Calculate new power using PV voltage and current
Pnew = Vpv*Ipv;
Dnew = 0; %because matlab and me disagree
Dstep = 0.01;

%Initial condition is D = 0.7 to get simulation started
if time < .1
    Dnew = 0.8;

%Increasing power, Increasing Voltage
%keep increasing volgate by decreasing duty cycle
elseif (time >= .1) && (Pnew >= Pold) && (Vpv >= Vold)
    Dnew = Dold - Dstep;

%Increasing power, Decreasing Voltage
%keep decreasing volgate by increasing duty cycle
elseif (time >= .1) && (Pnew >= Pold) && (Vpv <= Vold)
    Dnew = Dold + Dstep;
```

```
%Decreasing power, Increasing Voltage
%instead decrease volgate by increasing duty cycle
elseif (time >= .1) && (Pnew <= Pold) && (Vpv >= Vold)
    Dnew = Dold + Dstep;

%Decreasing power, Decreasing Voltage
%instead increase volgate by decreasing duty cycle
elseif (time >= .1)&& (Pnew <= Pold) && (Vpv <= Vold)
    Dnew = Dold - Dstep;
end

%set the olds
Pold = Pnew;
Vold = Vpv;
```

```
end
```

Appendix I: Additional Research

The following pieces of information are results of research conducted for the project that were later discarded due to a number of reasons. Among them there was not enough time for the implementation.

GPS

EVA-M8

For the development of this project, we had chosen to use the u-blox EVA-M8 GNSS module. The EVA-M8 is designed by u-blox, the same company that designs the RPMA chip, we will discuss in the next section. The EVA-M8 is:

- Designed to work with the four constellations
- Has a 16 Mbit SQI flash memory
- It interfaces through UART, USB and/or SPI
- It comes in two configurations M8M and M8Q. The M8M configuration has crystal oscillator for lower system costs while the M8Q has a TCXO (Temperature Compensated Crystal Oscillator for better performance.

Wireless (RPMA)

RPMA or Radio Phase Multiple Access is a wireless technology that was designed especially for machine-to-machine communication. RPMA works in the 2.4GHz broadcast frequency and functions bidirectional. The 2.4 GHz frequency band it uses was determined as the Industrial, Scientific and Medical radio bands. This band is not regulated; anyone can have devices transmitting at this frequency, for example, WIFI or hand-free home phones use this spectrum.

RPMA access is dependent on RPMA access points. Access points are antennas that receive and transmit data to RPMA devices. Access points can have very high coverage, of up to 300 square miles. For example, Dallas/Fort-Worth metropolitan area, of about 9300 square miles and 6.3 Million inhabitants, is covered with only 17 access points. This makes RPMA cost-effective in its deployment.

RPMA access points can offer a transmission throughput of 19,000 bps/MHz. this capacity is unparalleled in range and capacity to its competitors including LPWA, Cellular, WIFI, Bluetooth, SigFox.

	Sigfox	LoRa	EC-GSM-IoT	NB-IoT	LTE Cat-M1	RPMA
Bandwidth	100Hz	125kHz	600kHz	180kHz	1.08MHz	1MHz
Coverage	149dB	157dB	164dB	164dB	160dB	177dB
Capacity	50,000/cell	40,000/cell	190,000/cell	200,000/cell	1M/cell	500,000/cell
Battery Life	10 years +	10 years +	10 years +	10 years +	10 years +	10 years +
Throughput	100bps	290bps - 50kbps	473kbps	250kbps	1Mbps	624kbps
2-Way Data	No	Class dependent	Yes	Yes	Yes	Yes
Security	16bit	32bit	3GPP (128-256bit)	3GPP (128-256bit)	3GPP (128-256bit)	AES 128bit
Scalability	Low	Medium	High	High	High	High
Mobility Support	No	Yes	Idle Mode	Idle Mode	Connected+Idle Mode	Yes
Location Support	No	Yes	Needs GPS	Needs GPS	Needs GPS	Needs GPS

Figure 42 – Wireless Technologies Comparison

Access Point

In order to receive the signal that the RPMA module sends there needs to be an access point. This access point are sold and/or rented by Ingenu, a company that specializes in RPMA technology. For this project we are seeking to obtain an access point from Ingenu and place it on the WPI campus. Hence allowing for the development of other RPMA technologies.

RPMA Module - NANO S-100

The Nano S-100 RPMA module will be used in our device to transmit the data to the access point. The NANO S-100 has a 4-wire SPI interface. This module displays very low power consumption, for applications needing 10 years or longer battery life. It can transmit up to 100 kB daily.

Microcontroller

For a microcontroller we have chosen the TI - MSP430FR4133. For the development phase, we will be using the Launchpad format of this microcontroller, later on we expect to create a PCB board with the microcontroller. The MSP430FR4133 features:

- 16-bit MCU
- 16 kB of nonvolatile FRAM
- 10-channel 10-bit ADC
- Serial Interfaces (SPI, UART, I²C)

This microcontroller is suited to handle all of the different components in our design. We will be using five ADC channels, one for each SPEC sensor. UART interface for the PM Sensor. Then the SPI interface to communicate with the RPMA module (Nano S-100). And last I²C for the GNSS module (EVA-M8M).